CERN-ACC-2017-0101

December 12, 2017

davide.gamba@cern.ch

Beam dynamics requirements for HL–LHC electrical circuits

D. Gamba, G. Arduini, M. Cerqueira Bastos, J. Coello De Portugal, R. De Maria, M. Giovannozzi, M. Martino, R. Tomas Garcia
CERN, CH-1211 Geneva 23, Switzerland

Abstract
A certain number of LHC magnets and relative electrical circuits will be replaced for the HL-LHC upgrade. The performance of the new circuits will need to be compatible with the current installation, and to provide the necessary improvements to meet the tight requirements of the new operational scenario. This document summarises the present knowledge of the performance and use of the LHC circuits and, based on this and on the new optics requirements, provides the necessary specifications for the new HL-LHC electrical circuits.

Keywords
LHC, HL–LHC, circuit specifications, power converters

Contents

1 Introduction

The High Luminosity LHC (HL–LHC) project [1] foresees the replacement of several magnets, mainly in the low-beta insertions (IR1 and IR5). The scope of HL-LHC is to increase the instantaneous luminosity by increasing the bunch population, by reducing the beam size at the interaction point and by using crab cavities in order to maximise the overlap volume of the colliding bunches. Both improvements require a fine tuning of the beam parameters. This translates in cutting-edge performance requirements of all systems, in particular for the new magnets and related electrical circuits. The ultimate goal of HL–LHC is to increase the integrated luminosity, which strongly depends on the operational efficiency and, among other, by the turnaround time. This is an important aspect to keep in mind while considering the specifications and the redundancy of the new installations. Any risk of downtime due to malfunctioning hardware should be minimised, and each beam manipulation should be concluded safely without triggering undesired beam dumps. This also requires to allow reasonable margins in order to tolerate possible non conformities that may occur.

In HL–LHC a few magnets and circuits, mainly in the insertion regions around LHC P1 and P5, will be completely renewed. The performance of these new type of magnets and of the novel circuit configurations must be compatible with those LHC magnets and circuits that will remain unchanged. As a starting point, the design specifications of the LHC circuits and their use is analysed in Section 2. Based on this and on additional considerations, the specifications of the new HL–LHC circuits are presented in Sections 3 and 4.

2 Circuits in LHC

In the LHC Design Report [2] the following definitions are used:

- Nominal current (I_{nom}): Current for 7 TeV operations corresponding to 8.33 T main dipole field.
- Rated current (I_{rated}): Maximum current of the Power Converter (PC).
- Minimum current (I_{min}): Minimum current delivered by unipolar PC.
- Calibration current ($I_{calibration}$): Calibration value = software decided maximum current ($\leq I_{rated}$).
- Overload Current ($I_{overload}$): A hardware protection setting, corresponding to tripping the converter if exceeded.
- Ultimate current ($I_{ultimate}$): Current required for 7.5 TeV operations or 9 T main dipole field.

For PCs with $I_{nom} > 1$ kA the following relations are specified:

$$I_{calibration} = I_{nom} \tag{1}$$

$$I_{overload} = 1.1 \times I_{calibration} = 1.1 \times I_{nom} \approx 1.03 \times I_{ultimate} \tag{2}$$

while for PCs with $I_{nom} < 1$ kA it was chosen to be:

$$I_{nom} = I_{ultimate}. \tag{3}$$

The same definitions and conventions should be applied for the new HL–LHC circuits. The latest relation however might lead to confusion and it will *not* be used in this document. Instead for all circuits, independently of I_{nom}, it is assumed:

$$I_{ultimate} = 1.08 \times I_{nom}. \tag{4}$$

The same convention is presently used in [3]. Clearly, the final specification of all circuits will need to sustain the more demanding performances associated to $I_{ultimate}$.

Besides the maximum current that each circuit needs to sustain, it is important to also specify the maximum ramp rates, maximum acceleration rates and the stability that are necessary for a successful handling of the beam during all phases of a fill. In the following sections the present LHC circuits ramp rates and stability performance are analysed and summarised.

2.1 Ramp rates of the LHC circuits

Each circuit in the LHC must be commissioned before starting beam operations. An overview of the powering specifications for Run 2 is available in [4], from which the relevant ramp rates are reported here in Table 1. Note that the nominal current (I_{nom}) is what specified in [2], while the ramp rates might be slightly different than what presently specified in the CERN Layout Database [5] or in earlier versions of similar documents, e.g. in [6]. The values reported in Table 1 are the result of a few year experience of LHC operation, and they are here considered as the starting point for defining the ramp rates for the new power converters. It has to be stressed that the values currently established might not reflect the original specifications or expectations. The fact that the present values are sufficient for allowing the present LHC operations, does not necessarily mean that they represent actual hardware limitations or that they cannot be overcome if required. For example octupoles (ROD and ROF circuits) are presently powered up to 590 A instead of the 550 A initially foreseen. Note that a list of known issues for different circuits is presently available in [7].

2.2 Typical operations of the present LHC circuits

The following figures refer to the Proton fill #5848 which was played on June 19$^{\text{th}}$ 2017. The nominal beam energy was 6.5 TeV, while the optics implemented in the machine was an ATS optics [8] with β^*

Table 1: Ramp and acceleration rates used for powering tests of some LHC superconductive circuits relevant to the present discussion [4].

Circuit name	I_{nom} **[A]**	**Ramp rate [A/s]**	**Acceleration [A/s^2]**
RB	11850	10	1
RQ(D/F)	11870	10	1
RS(D/F/S)	550[a]	1.5	0.15
RO(D/F)	550[a]	5	0.1
RQS[b]	550	1.5	0.1–0.2
RQT[b]	550	1.5–5	0.1–0.5
RQX (IR1, IR5)	6800	6.2	1
RQX (IR2, IR8)	7180	6.8	1
RTQX1 (IR1, IR2, IR5, IR8)	550	1.5	0.1
RTQX2 (IR1, IR5)	4600	4	1
RTQX2 (IR2, IR8)	4780	6	1
RQ4 (IR1, IR2, IR5, IR8)	3610	10.833	2
RQ5 (IR1, IR5, R2, L8)	4310	12.931	2
RQ5 (L2, R8)	3610	10.833	2
RQ6 (IR1, IR2, IR5, IR8)	4310	12.931	2
RQ7-10	5390	16.167	2
RD2 (IR1, IR5)	4670	12.972	2
RD2 (IR2, IR8)	6500	18.147	2
RCBX	540	2.5	0.2
RC(O/S/T)X	100	0.5	0.25
RCBY(H/V)(4-5)	72	0.667	0.25
RCBC(H/V)(5-6)	80	0.667	0.25
RCBC(H/V)(7-10)	100	1	0.25

[a] Despite I_{nom} is specified to be 550 A in [2], in [4] this has been reduced to 500 A or increased to 590 A for different circuits due to non conformities or optics requirements.

[b] According to [4] many RQT circuits are tested for different ramp and acceleration rates mainly because of non conformities (See [7]).

of 40 cm in IP1 and IP5, 10 m in IP2 and 3 m in IP8. During stable beam operations crossing angle levelling was successfully performed a few times in IP1 and IP5.

The data used for the following plots and analysis has been extracted from the Timber logging database. The ramp and acceleration rates have been computed by numerical differentiation.

2.2.1 Energy ramp

Figure 1 shows the current measured in a few relevant circuits during the energy ramp of the LHC. From the speed and acceleration plots one can clearly see the squeeze which starts approximately at one third of the ramp and it lasts until the end of the energy ramp. The fastest circuit is that of the main bending magnets, with ramp-up rates of 10 A/s just before reaching the value of 10979 A equivalent to ≈ 6.5 TeV operation with protons. The nominal current for the main bending magnets is $I_{nom} = 11850$ A (see Table 1), therefore a possible scaling factor k for defining the ramp rates of the new circuits could be the ratio:

$$k = \frac{\text{Max ramp rate bends}}{I_{nom}\text{ bends}} = \frac{10}{11850}, \tag{5}$$

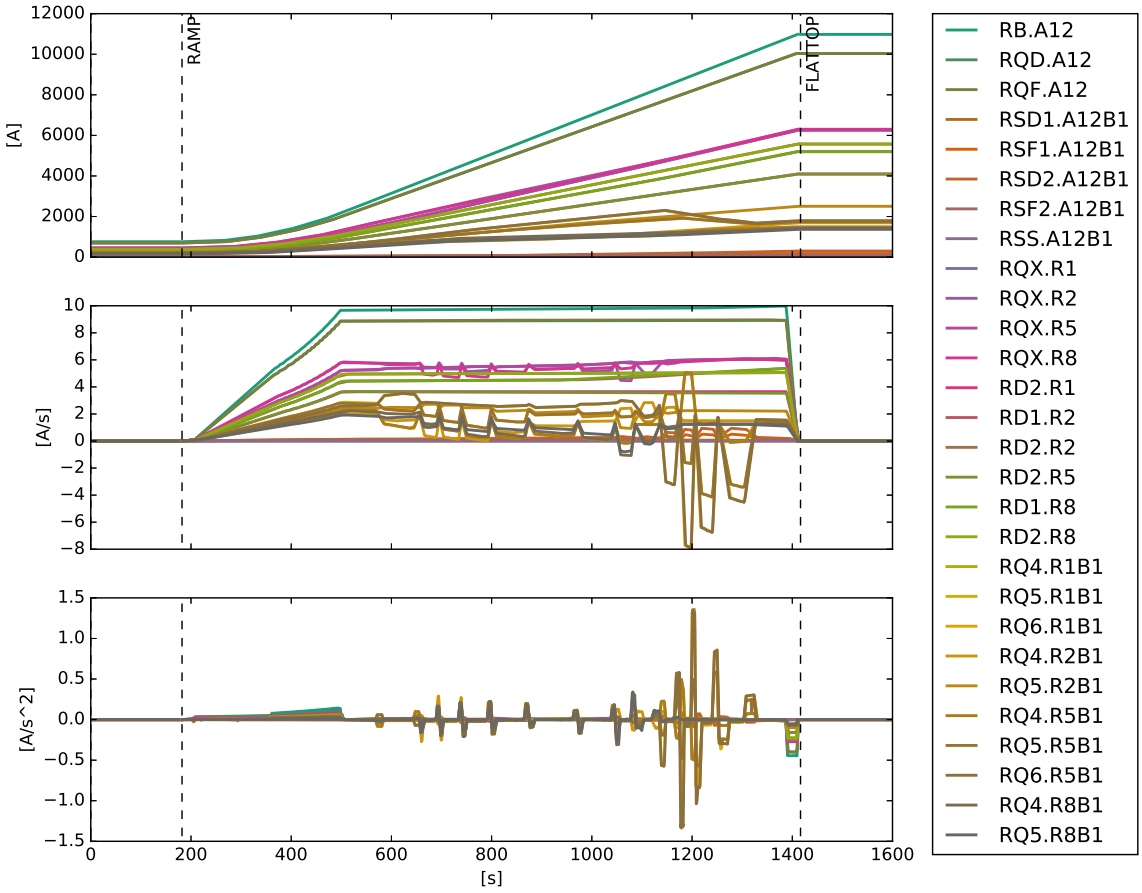

Fig. 1: Typical PRERAMP, RAMP, FLATTOP beam processes for a few main circuits in LHC. The top figure is the measured current in the circuits as a function of time. The middle and bottom figures are the first and second time derivatives numerically computed, respectively. The vertical dashed lines delimit the different beam processes.

such that

$$\text{Max ramp rate new circuit} = k \times (I_{nom} \text{ new circuit}). \tag{6}$$

The same scaling law could be used for computing the new acceleration rates:

$$\text{Max acceleration new circuit} = \frac{\text{Max acceleration bends}}{I_{nom} \text{ bends}} \times (I_{nom} \text{ new circuit}) \tag{7}$$

$$= \frac{1}{11850} \times (I_{nom} \text{ new circuit}). \tag{8}$$

Note that the triplets and matching sections quadrupoles are not necessarily used at their I_{nom} current, but they are powered according to the optics needed for the different phases of the machine cycle. As an example, the RQ5.R5B1 circuit reaches the maximum current of approximately 2600 A during the analysed fill, while its I_{nom} is 4310 A (see Table 1). One would then need to consider the actual optics and its implementation in the machine (i.e. the squeeze) for defining the actual ramp rates of the new quadrupole circuits. Moreover one should expect that the optics will not be fixed but it will rather evolve with the experience matured and with the new needs expressed by the experiments. Therefore, enough margin on the ramp rates has to be ensured to allow for a comfortable manipulations of the optics.

Currently the energy ramp takes approximately 1200 s to reach 6.5 TeV (see Fig. 1). Assuming to extend the ramp at maximum speed (e.g. 10 A/s for the main dipoles) one would need additional 87 seconds to reach the nominal current of 11850 A in the main dipoles (7 TeV) and additional 95 seconds to reach the ultimate current 11850×1.08 A. With the present LHC one can then estimate the nominal and ultimate ramp-up times to be about 1300 s and 1400 s, respectively.

Figure 1 shows that at the beginning of the ramp the circuits are gently increased in speed in about 300 s, while the end of the ramp is terminated in about 20 s. This is consistent with the Parabolic-Exponential-Linear-Parabolic (PELP) ramping scheme [9].

2.2.2 Ramp down

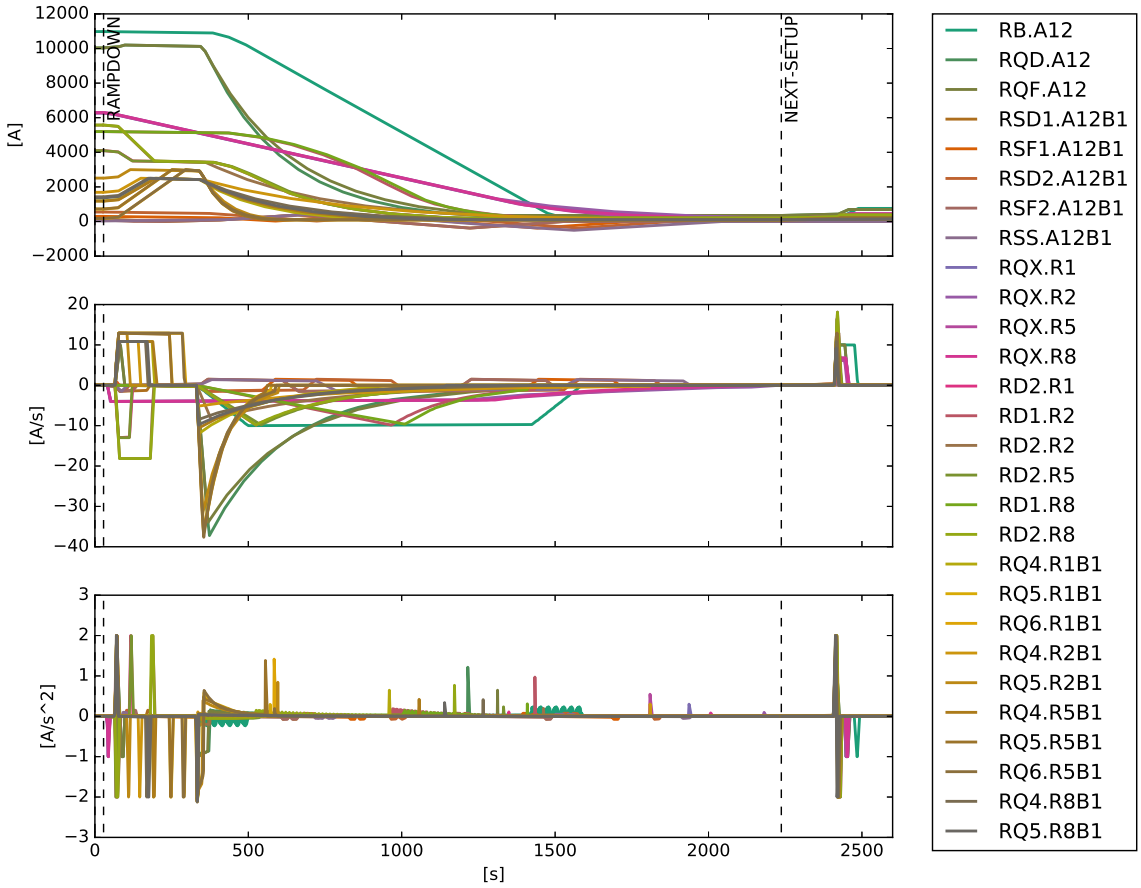

Fig. 2: Typical BEAMDUMP, RAMPDOWN and the following SETUP sequence for a few main magnets in LHC. The top figure is the measured current in the circuits as a function of time. The middle and bottom figures are the first and second time derivatives numerically computed, respectively. The vertical dashed lines delimit the different beam processes.

Figure 2 shows the evolution of the measured currents during the ramp down from stable beam at 6.5 TeV. This process does not require high precision because is clearly performed without beam. Many circuits decay in "free" discharge from their latest setting. Others are brought first to a predefined current before starting the discharge. A zoomed version is proposed in Fig. 3, from which one can better estimate the type and duration of the ramp down. Table 2 summarises the main parameters of the current functions during the ramp down.

The triplet are the slowest circuits, RQX.R2 being the slowest with a total ramp down time of about

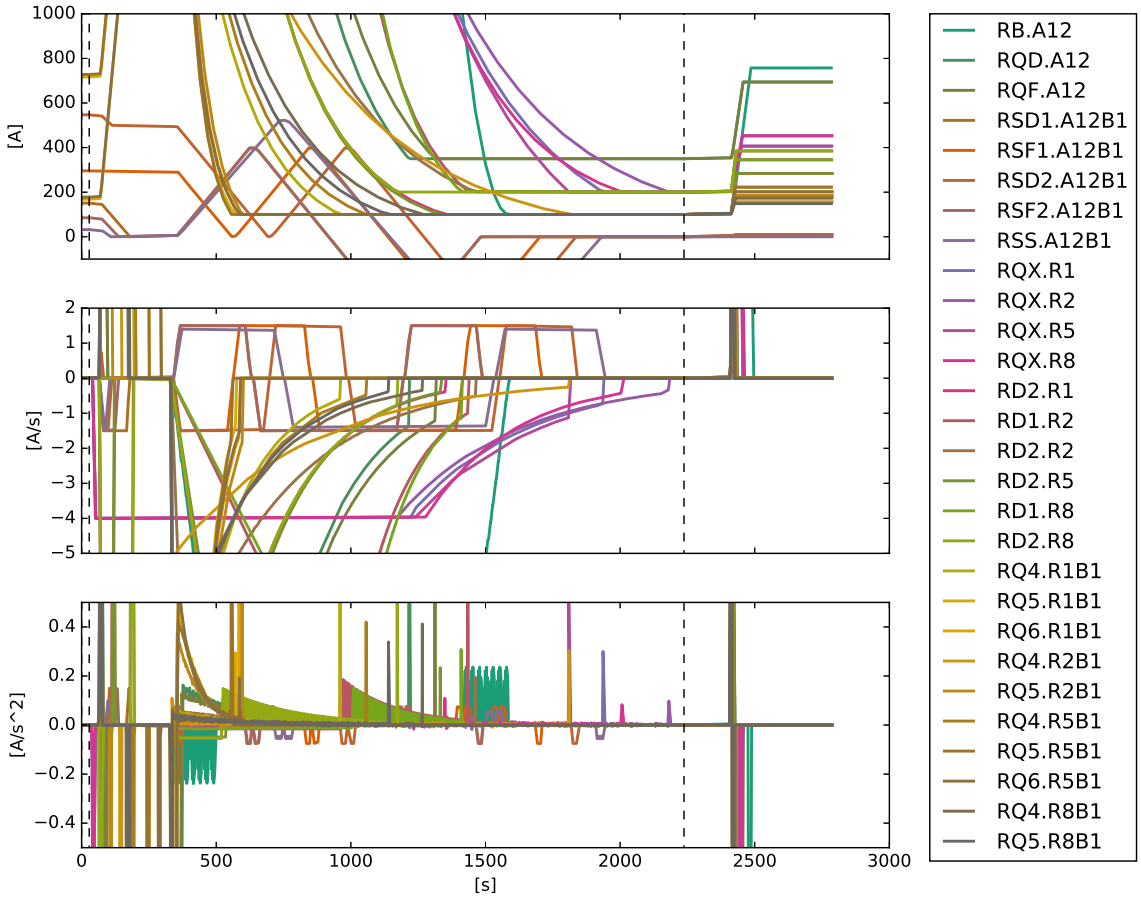

Fig. 3: Zoom in of Fig. 2.

2122 s. The triplets of IR1 and IR5 ramp down in less than 1900 s. The main bends and quadrupoles, as well as the matching section magnets, ramp down in the shadow of the main dipoles, taking 1217 s. Exception is RQ4.R2B1 which takes about 1468 s to ramp down. Note that approximately 400 s are needed for ramping up the matching quadrupoles to predefined values before the actual ramp down, e.g. RQ6.R1B1 is brought first from 168 A to 3000 A before actually starting its discharge. This procedure has been put in place to improve the repeatability of the magnetic field, profiting of the long discharge time of IR2 and IR8 triplet. This time is also used to bring most of the 600 A circuits to a predefined value before starting the degaussing cycles [10]. Examples are the sextupoles, RS(D/F/S), that in Fig. 3 experience a triangular-shape cycle. It might be possible, with the necessary changes on the PC controls, to reduce the length of those cycles if the ramp-down time of all the IR triplets will be reduced in HL–LHC [10, 11].

2.2.3 Maximum ramp and acceleration rates

The maximum and minimum values for current and ramp rates observed during fill #5848 are summarised in Table 3. The values are divided between processes with beam (INJPROT, INJPHYS, PRERAMP, RAMP, FLATTOP, SQUEEZE, ADJUST, STABLE) and without beam (BEAMDUMP, RAMPDOWN, SETUP). A comparison of the different processes divided by circuit type is also available in Appendix A. Note that the sampling frequency of the data used for the analysis is 2 Hz, therefore faster changes are not detectable here.

Table 3 shows that the maximum and minimum ramp rates are exploited during the SETUP and

Table 2: Circuit absolute current at beam dump, at start and end of the ramp down and total ramp-down time for the main circuits in LHC as measured during fill #5848.

Circuit name	I **at beam dump [A]**	I **at start ramp down [A]**	I **at end ramp down [A]**	**Ramp down time [s]**
RB.A12	10979	10980	100	1217
RQD.A12	10035	10200	350	873
RQF.A12	10036	10200	350	970
RQX.R1	6271	6271	200	1885
RQX.R2	6298	6298	200	2122
RQX.R5	6270	6269	200	1760
RQX.R8	6297	6297	200	1948
RD2.R1	4095	4095	100	1272
RD1.R2	5197	5200	200	1076
RD2.R2	5571	5571	200	1386
RD2.R5	4097	4097	100	1254
RD1.R8	5200	5200	200	1051
RD2.R8	5575	5575	200	1098
RQ4.R1B1	1195	2500	100	623
RQ5.R1B1	717	3000	100	237
RQ6.R1B1	168	3000	100	250
RQ4.R2B1	1688	2500	100	1468
RQ5.R2B1	2509	3000	100	262
RQ4.R5B1	1176	2500	100	719
RQ5.R5B1	728	3000	100	221
RQ6.R5B1	178	3000	100	252
RQ4.R8B1	1430	2500	100	926
RQ5.R8B1	1367	2500	100	801

RAMPDOWN processes. The energy ramp and the optics gymnastic during the squeeze also require fast ramp-up rates. The speed of the D1 and D2 dipoles, as well as the corrector circuits, is also dominated by the SETUP and RAMPDOWN processes when degauss cycles are performed for some of these circuits.

Figure 4 shows the use of the orbit correctors during the beginning of the analysed fill. For the whole duration of the beam cycle the LHC orbit feedback [12] is active in order to keep the orbit close to the "golden" orbit defined by the operators. Due to the tight constraint imposed by the Quench Protection System (QPS), the RCBX correctors are not used by the orbit feedback in order to avoid undesired beam dumps triggered by the QPS [13]. During STABLE-beam operations the orbit correctors are also used for luminosity optimisation. The histograms of orbit corrector current deviation from average and speed used during STABLE beam in fill #5848 are reported in Appendix B. Note that from the LHC experience the actual bandwidth of the feedback is about 0.1 Hz and the average kick rate required by the feedback is approximately 0.2 μrad/s [14]. The maximum kick rate that can be provided by the LHC correctors is about 1 μrad/s at 7 TeV.

Table 3: Maximum current and maximum/minimum ramp and acceleration rates exploited during fill #5848 at 6.5 TeV on the main circuits (RB, BQ(D/F), RS(D/F/S)) and on the main superconducting circuits of P1 and P5.

Circuit name	**Max I [A]**		**Min / max ramp rate [A/s]**		**Min / max acc. [A/s^2]**	
	w/o beam	with beam	w/o beam	with beam	w/o beam	with beam
RB	10980	10979	-10.00 / 10.00	0.00 / 9.98	-1.00 / 1.00	-0.45 / 0.15
RQ(D/F)	10200	10036	-37.27 / 10.00	0.00 / 8.96	-1.06 / 1.22	-0.40 / 0.13
RS(D/F/S)	547	548	-1.50 / 1.50	-0.11 / 1.09	-0.15 / 0.15	-0.11 / 0.11
RO(D/F)	508	508	-5 / 5	-1.31 / 1.31	-0.10 / 0.10	-0.10 / 0.10
RQS	380	96	-1.4 / 1.5	-0.18 / 0.20	-0.2 / 0.2	-0.10 / 0.10
RQT	523	189	-1.5 / 5	-0.98 / 0.25	-1 / 1	-0.13 / 0.13
RQX	6273	6273	-4.02 / 6.20	0.00 / 6.10	-1.00 / 1.00	-0.27 / 0.09
RTQX1	0	4	-0.10 / 1.50	-0.24 / 0.11	-0.10 / 0.10	-0.02 / 0.02
RTQX2	4333	4336	-3.50 / 4.00	-0.04 / 4.00	-1.00 / 1.00	-0.16 / 0.06
RQ4	2500	1482	-27.05 / 10.83	-2.10 / 6.60	-2.15 / 2.00	-0.71 / 0.70
RQ(5/6)	3000	2313	-40.57 / 12.93	-8.46 / 3.62	-2.09 / 2.20	-1.40 / 1.42
RD2	4097	4097	-12.97 / 12.97	0.00 / 3.65	-2.00 / 2.00	-0.16 / 0.06
RCBX	400	256	-2.60 / 2.60	-1.07 / 0.63	-0.38 / 0.38	-0.20 / 0.20
RC(O/S/T)	95	38	-0.50 / 0.50	-0.08 / 0.10	-0.25 / 0.25	-0.09 / 0.09
RQSX	400	162	-1.50 / 1.50	0.00 / 0.14	-0.10 / 0.10	-0.01 / 0.01
RCBY	68	22	-0.69 / 0.69	-0.63 / 0.44	-0.66 / 0.64	-0.20 / 0.20
RCBC(5/6)	76	22	-0.69 / 0.69	-0.50 / 0.28	-0.41 / 0.31	-0.15 / 0.15

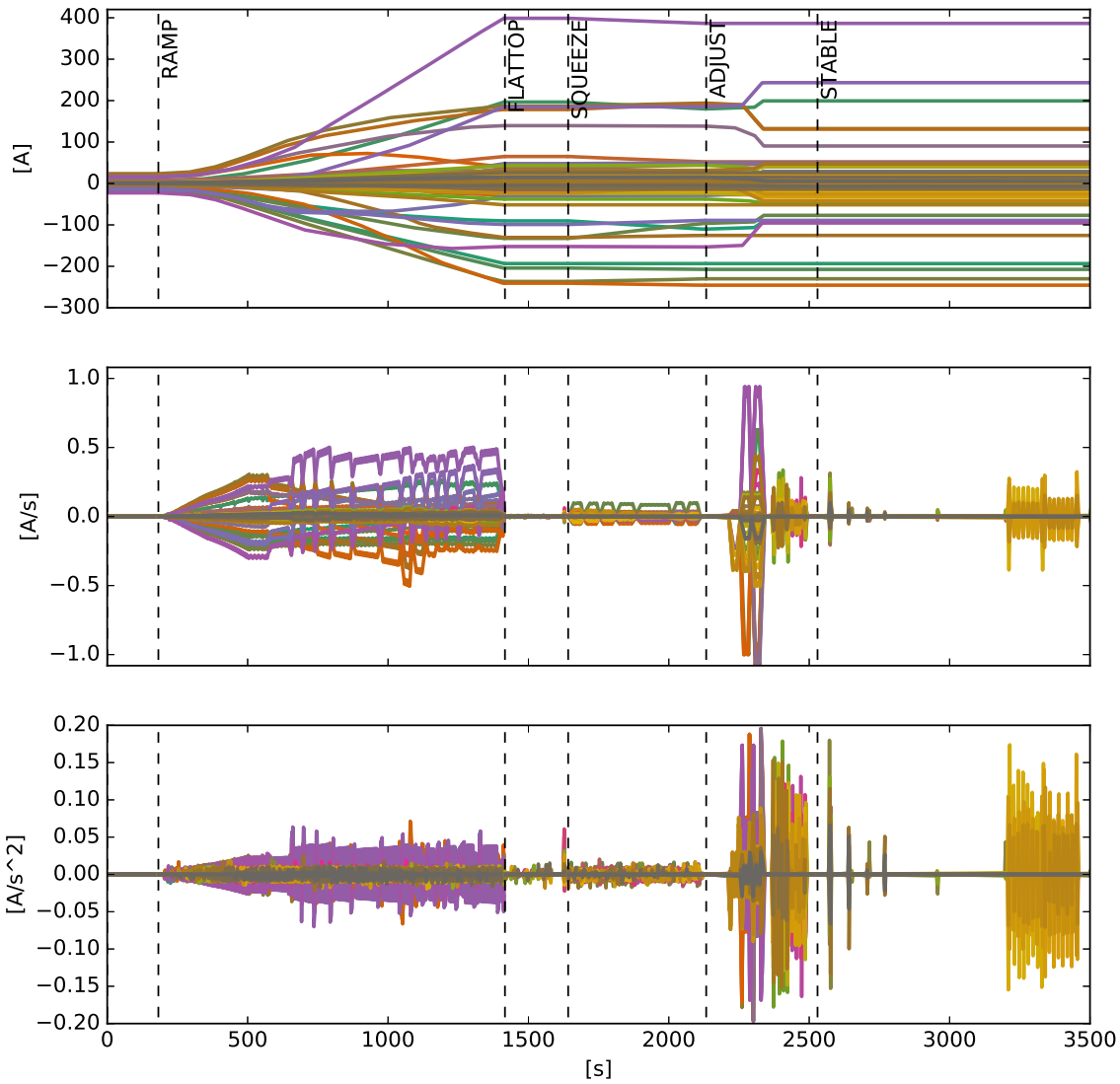

Fig. 4: Typical PRERAMP, RAMP, FLATTOP, SQUEEZE, ADJUST, and beginning of STABLE beam processes for all orbit correctors in all IRs and matching sections up to Q6. The top figure is the measured current in the circuits as a function of time. The middle and bottom figures are the first and second time derivatives numerically computed, respectively. The vertical dashed lines delimit the different beam processes.

2.3 LHC circuits current uncertainty

Another important specification defined in [2] is the current uncertainty[1] of the PCs, which is given with respect to the following quantities expressed in ppm of I_{rated}:

- **Accuracy**: long-term uncertainty (over a period of 1 year). It was specified that this could be improved/relaxed by regular in-situ quasi-on-line calibrations to be performed, for example, every month[2].
- **Reproducibility**: fill-to-fill current uncertainty (period of 1 day without calibrations).
- **Stability**: maximum deviation from the settings over a period of half an hour.
- **Resolution**: smallest increment in current that can be induced or discerned.
- **Tracking**: ability of the PC to follow a reference function.

Both dynamic and static imperfections fall under the "tracking" definition. The static part is covered by the accuracy and reproducibility definitions. The dynamic part is mainly due to timing and lagging errors.

One of the main concerns in [2] was the tracking error between the eight main dipole PCs and between the main dipole and main quadrupole PCs. From the estimations in [2], it was expected about 0.7 mm beam orbit error in the arcs and 0.033 tune shift. Both errors were assumed to be cured by using a pilot beam and so by adjusting the bends' strength and correcting the tune with tuning quadrupoles (which were assumed to be able to correct the tune up to 0.3 units). Moreover, during the energy ramp, assuming 10 A/s ramp rate and 13000 A I_{rated}, it was calculated that 1 ms timing synchronisation between the different circuits was sufficient to limit the contribution of timing to dynamic errors to less than 1 ppm. In order to achieve this specification, a communication infrastructure between PCs was developed, able to fulfill the 1 ms synchronisation requirement with a time stability of a few μs [16].

The relevant conclusions of [2] were that "the accelerator physics requirements translate into an overall high precision [17]" and that the performance of the powering system is dominated by the tune tolerance (0.003 for the LHC)[3]. Moreover, the resolution and the stability of the PCs was required to be of the order of a few 10^{-6} in order to allow precise cycling and fine adjustment.

From the above considerations the Dynamic Effects Working Group recommended the specifications summarised in Table 4. The power converters voltage ripple was also specified at the main frequencies of 50, 300 and 600 Hz for the different type of converters with values from 5 mV at 50 Hz up to 3000 mV at 600 Hz for some PCs [2].

The actual performance of the PCs installed in the LHC is better than what specified in Table 4 [19, 20], moreover the inner triplets are currently powered with the same PC class as the main dipoles and quadrupoles. The experience gathered in the LHC and the actual needs for HL–LHC operation suggested different quantities to be used to specify the required performance of the PCs. Following ongoing discussions with WP6b [15, 21], the following new definitions are used in this document to characterise the PC uncertainties:

- **Setting resolution**: smallest step in current that can be induced and discerned.
- **Initial uncertainty after calibration**: deviation of the delivered current with respect to an accepted current reference. This quantity can be used to estimate the relative calibration error between different circuits.
- **Linearity**: maximum deviation, in absolute value, of the delivered current from the requested current along the whole setting range from $-I_{rated}$ to $+I_{rated}$ (or from I_{min} to I_{rated} for unipolar PCs).

[1] Note that in previous documents as well as in the LHC Design Report [2] this was referred as "circuits precision".

[2] In practice, the periodicity of the calibrations turned out to be of 6 months [15].

[3] This comes from considerations summarised in [18] where it is also stated that "Orbit excursions should be limited to less than 0.5 mm (r.m.s. of the closed orbit)", and "the chromaticity should be limited to some units".

Table 4: Required precision (peak-to-peak allowed excursion w.r.t. I_{rated}) of the LHC circuits [2].

Circuit Type	I_{rated} **[A]**	**Current Polarity**	**One Year Accuracy**	**One day Repro-ducibility**	**1/2 hour Stability**	**Resolution**
Main bends, main quads	13000	Unipolar	± 50 (± 20 with cal.)	± 5	± 3	1
Inner triplet[a]	8000/ 6000	Unipolar	± 100 (± 20 with cal.)	± 20	± 10	15
Insertion quadrupoles	4000/ 5000/ 6000	Unipolar	± 70	± 10	± 5	15
Cold separation dipoles (D1, D2, D3, D4)	5000/ 7000	Unipolar	± 70	± 10	± 5	15
Trim quadrupoles, SSS correctors, Spool pieces	600	Bipolar	± 200	± 50	± 10	30
Orbit correctors	120/60	Bipolar	± 1000	± 100	± 50	30
Warm magnets	650/ 1000	Unipolar	± 200	± 50	± 10	15

[a] In the actual LHC the performance of the inner triplet PCs are the same as main bends and main quads [19].

- **Stability during a fill (12 h)**: maximum deviation, in absolute value, of the delivered current from the initial setting during a 12 hour-long fill. This parameter is mostly dominated by thermal effects, such as thermal settling of the control and measurement electronics. Flicker (1/f) noise can also contribute, albeit on a smaller scale. Such an effect can be approximated by a slow and monotonic variation the delivered current during a fill, and it can be either positive or negative for different PCs.
- **Short term stability (20 min)**: variation of the delivered current during 20 minutes stable setting after a 30 minutes-long thermal settling and with bandwidth from 0.001 to 0.1 Hz.
- **Noise (0.1-500 Hz)**: variation of the delivered current with bandwidth from 0.1 Hz to 500 Hz.
- **Voltage spectrum tones**: spectrum line amplitudes at 50 Hz, 150 Hz, 300 Hz, f_{sw}, $2 \times f_{sw}$, where f_{sw} is the switching frequency (normally of the order of a few kHz) used in the power converter. Those are the most likely tones where to expect high voltage ripple, but other tones might appear [15].
- **Fill-to-fill repeatability**: variation of the fill average current from fill to fill, measured over 10 consecutive fills.
- **Long term fill-to-fill stability**: maximum deviation, in absolute value, of the delivered current from the initial setting after one year from the last calibration. This implies many cycles of the PC. This parameter is mostly dominated by ageing of the control and measurement electronics, or flicker (1/f) noise. Such an effect can be approximated by a linear drift in the positive or negative direction of the delivered current along the year. The direction of the drift varies from PC to PC.

The different quantities are specified in ppm of I_{rated} as r.m.s. (with a certain coverage factor normally equal to 2) or as maximum deviation from the reference value. Table 5 provides the conditions of validity and units used for the different quantities, while Fig. 5 helps to visualise the different definitions. Note that the cycle shape in Fig. 5 is a simplistic representation of a single PC cycle, which is close only to the actual main dipoles and quadrupoles behaviour. Note that the "setting resolution", "initial uncertainty after calibration" and "linearity" are static figures, while "stability during a fill (12 h)" and "Long term fill-to-fill stability", although dynamic, have a deterministic behaviour over time (12 hours and 1 year, respectively).

Table 5: Bandwidth (BW), environment condition of validity, and units of the uncertainty definitions used in this document. The equivalent definition used for the LHC Design Report (DR) [2] is also reported. Units in ppm are given with respect to I_{rated}.

HL–LHC definition	**BW/Condition**	**Units**	**Equivalent LHC DR definition**
Setting resolution	n.a.	ppm	Resolution.
Initial uncertainty after cal.	1 mHz–100 mHz; $\Delta T_{amb} < 5$ C	2×r.m.s. ppm	n.a.
Linearity	n.a.	|.| max ppm	n.a.
Stability during a fill (12 h)	20 μHz–10 mHz; $\Delta T_{amb} < 5$ C	|.| max ppm	n.a.
Short term stability (20 min)	1 mHz–100 mHz; $\Delta T_{amb} < 2$ C	2×r.m.s. ppm	Stability (30min)
Noise (0.1-500 Hz)	100 mHz–500 Hz	2×r.m.s. ppm	n.a.
Voltage spectrum tones	> 10 Hz	r.m.s. mV	≈Voltage ripple
Fill-to-fill repeatability	$\Delta T_{amb} < 5$ C	2×r.m.s. ppm	Reproducibility (24h)
Long term fill-to-fill stability	$\Delta T_{amb} < 5$ C	|.| max ppm	Accuracy (1year)

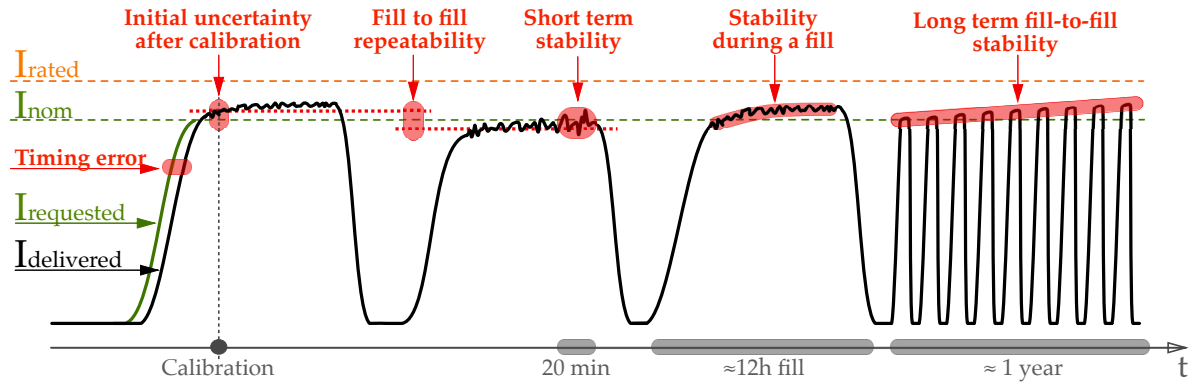

Fig. 5: Main uncertainty definitions introduced in this document highlighted on a sketch of many simple cycles of a single PC.

Note that the definition of "noise (0.1-500 Hz)" will not necessarily translate into a magnetic-field variation of the same amplitude seen by the beam. In fact, for frequencies above the regulation frequency (presently assumed to be 0.1 Hz) the inductance of the actual circuit (including the effect of the cold bore

and beam screen) becomes relevant.

According to the newly defined specifications, the power converters developed for LHC fall in the new classes specified in Table 6. The relevant circuit rated currents and classes are then summarised in Table 7. Note that no class 0 PC is presently installed in the LHC. Such a PC is the result of recent technological and design improvements, and it could be used for future installation or upgrades.

Table 6: Uncertainty specifications for the different classes of PCs installed in LHC (classes 1 to 4) and possibly available for future upgrades (class 0). The values are based on actual measurements and estimations [15, 21], and represent a single PC.

PC class:	**0**	**1**	**2**	**3**	**4**
Setting resolution [ppm]	0.5	0.5	1	1	1
Initial uncertainty after cal. [2×r.m.s. ppm]	2	2	5	10	20
Linearity [|.| max ppm]	2	2	5	10	10
Stability during a fill (12 h) [|.| max ppm]	1	2	5	10	20
Short term stability (20 min) [2×r.m.s. ppm]	0.2	0.4	1	2	5
Noise (0.1-500 Hz) [2×r.m.s. ppm]	3	5	10	15	25
Fill-to-fill repeatability [2×r.m.s. ppm]	0.5	1	2	5	10
Long term fill-to-fill stability [|.| max ppm]	10	10	20	50	100

For the main dipole and main quadrupole PCs a remote controlled calibration system was installed in LHC [22], which allows to reduce the "long term fill-to-fill stability" accordingly to the frequency of the calibrations over one year. For example, if a calibration is performed every six months, then the "long term fill-to-fill stability" can be reduced of approximately a factor 2.

The overall tracking error during the energy ramp up to 3.5 TeV was demonstrated to be below 1 ppm peak-to-peak within a single main circuit (e.g. RB.A81) and below 2 ppm peak-to-peak within different main circuits (e.g. within RQD circuits of sector 12 and sector 23) [22]. This confirms the ability of synchronising different circuits with a timing error below 1 ms, and that during the ramp one is dominated by the short term stability of the PCs, i.e. the timing jitter has no impact on tracking.

All voltage tone amplitudes are below what specified in the "CERN gabarit" reported in Fig. 6 [23].

2.4 Summary

In the LHC the speed of the energy ramp is mainly dictated by the performance of main bending magnets (10 A/s and 1 A/s^2). The nominal and ultimate ramp-up times have been estimated to be about 1300 s and 1400 s respectively.

For all circuits the most demanding beam process is the RAMPDOWN when all circuits are cycled and discharged as fast as possible in order to minimise the turnaround. Presently the triplets of IR2 and IR8 are the bottleneck in terms of ramp-down time (more than 2100 s for 6.5 TeV operations). With the exception of the IR triplets, all other magnets ramp down in less than 1500 s from 6.5 TeV operations.

The triplet orbit correctors are presently not used by the orbit feedback due to the presence, only for those orbit correctors, of a QPS that could mis-interpret the requests from the feedback as a false quench, and therefore trigger unnecessary beam dumps.

The precision of the LHC PCs turned out to be considerably better than what initially specified in the LHC design report. New quantities for better expressing the precision have been defined in the previous section. Those definitions identify five main classes of PCs described in Table 6. The present PC class of the relevant LHC circuits are summarised in Table 7.

Table 7: Rated current and PC uncertainty class for each LHC circuit relevant to the discussion [2, 5, 15, 21].

Circuit name	I_{rated} **[A]**	**PC class**
RB	13000	1
RQ(D/F)	13000	1
RS(D/F/S)	600	3
RO(D/F)	600	3
RQS	600	3
RQT	600	3
RQX (IR1, IR5)	8000	1
RQX (IR2, IR8)	8000	1
RTQX1 (IR1, IR2, IR5, IR8)	600	3
RTQX2 (IR1, IR5)	6000	1
RTQX2 (IR2, IR8)	6000	1
RQ4 (IR1, IR2, IR5, IR8)	4000	2
RQ5 (IR1, IR5, R2, L8)	6000	2
RQ5 (L2, R8)	4000	2
RQ6 (IR1, IR2, IR5, IR8)	6000	2
RQ7-10	6000	2
RD2 (IR1, IR5)	6000	2
RD2 (IR2, IR8)	8000	2
RCBX	600	3
RC(O/S/T)X	120	4
RCBY(H/V)(4-5)	120	4
RCBC(H/V)(5-6)	120	4
RCBC(H/V)(7-10)	120	4

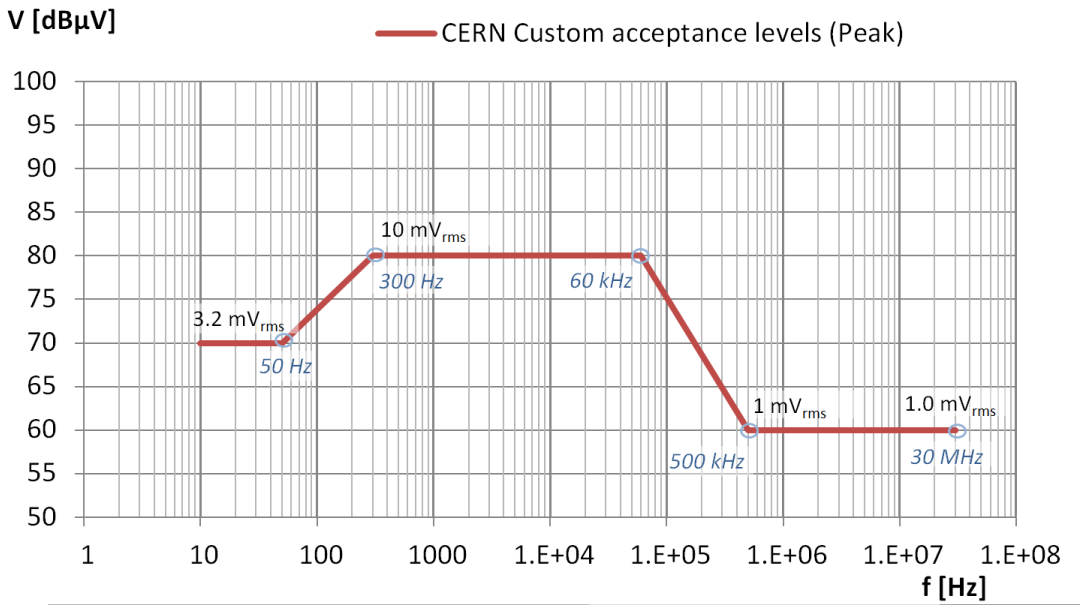

Fig. 6: CERN Output Side Gabarit (< 50 V dc output) [23]. The solid line is the maximum tolerated r.m.s. voltage ripple for a given frequency.

3 Ramp rates for the new power converters of HL–LHC

The main circuits that will be affected by the HL–LHC upgrade can be divided in three families: the triplets of point 1 and 5 with the associated linear and non-linear correctors, the matching section quadrupoles of these IRs and the introduction of two 11 T dipoles at each side of point 7 for allowing the installation of an additional collimator (TCLD). The electrical scheme of the new circuits is reported in Appendix C.

The triplets' normalised strength is changing slightly by 4 to 6% during the pre-squeeze. Most of the independently powered quadrupoles are used to implement the low-beta optics, and they require a substantial variation of their normalised strength during the transition from the injection to collision optics. For those magnets the nominal ramp rates should be defined according to the nominal optics, but one should keep enough margin to be able to implement alternative optics that might be required by the experiments. One needs to keep in mind that the pre-squeeze process starts already during the ramp in the so called "ramp and squeeze" scheme, which is currently in use in the LHC and is the baseline for HL–LHC [1].

The 11 T magnets will be powered in series with the main dipoles circuit, but they will need an additional trim to allow for the compensation of the different transfer function.

The different processes are analysed in more detail in the following sections.

3.1 Nominal ramp rates for the energy ramp

For the LHC main bending magnets the nominal current is I_{nom} = 11850 A, and their nominal ramp rate is 10 A/s (see Table 1). This is also the maximum ramp rate currently reached in the LHC during the energy ramp (see Table 3). The new inner triplets quadrupoles will be powered with nominal current of 16470 A. By simple scaling law, Eq. (6), the nominal ramp rate for these circuits needs to be $16470 \times 10/11850 = 13.90$ A/s in order to follow the energy ramp. The same argument can be applied for the separation and recombination dipoles D1 and D2 (I_{nom} = 12000 A), which gives 10.13 A/s.

For the matching section quadrupoles the nominal ramp rates depend on the actual beam optics and in particular on the adopted squeeze strategy as shown for the LHC in Section 2.2.1. To be noted that Q4 and Q5 of IR1 and IR5 will be of the same MQY type as the present Q4, but they will be cooled down to 1.9 K instead of 4.5 K as in the present LHC. The lower temperature will increase their maximum strength. Using the same scaling law used above and by considering the maximum strength as a target at the end of the ramp, one obtains 3.81 A/s for Q4 and Q5 (new I_{nom} = 4510 A). No hardware interventions are foreseen for the other quadrupoles in the matching sections. Additional considerations on the squeeze process are presented in Section 3.2.

The only relevant "nominal" process involving the linear orbit correctors is the crossing and separation scheme. The crossing and separation knobs – presented in [24] – are summarised in Table 8. One can consider the maximum strength required for either crossing or separation knobs and compute the nominal ramp rates during the energy ramp as:

$$(\text{Corrector ramp rate}) = (I_{nom}\ \text{corrector}) \times \frac{\left(\int B_{crossing}\mathrm{d}l\ \text{corrector}\right)}{\left(\int B_{nom}\mathrm{d}l\ \text{corrector}\right)} \times \frac{(\text{nominal ramp rate main bend})}{(I_{nom}\ \text{main bend})} \tag{9}$$

where $B_{crossing}$ is the magnetic field required in the corrector for the crossing scheme at nominal energy. Following Eq. (9), one would expect $1600 \times 2.12/4.5 \times 10/11850 = 0.64$A/s for the RCBX3, and similarly 0.23 A/s for RCBRD4 and 0.02 A/s for RCBY4. However from the LHC experience we know that the orbit feedback intervenes frequently during the energy ramp on the correctors of the matching sections [25]. It is also assumed that the IR correctors will also be included in the orbit feedback in HL–LHC. For those reasons only rough estimates are provided for corrector circuit nominal currents and ramp rates. Instead, the maximum ramp rates are discussed in Section 3.4.

Table 8: Necessary integrated strength necessary to implement the crossing scheme knobs for IP1/5 at 7 TeV, to be compared with the max strength/current of the correctors involved [24]. Here it is assumed the conservative value of ± 295 μrad for the half crossing angle instead of the ± 250 μrad nominal value.

Circuit name	**Half-crossing (± 295 μrad) [Tm]**	**Half-separation (± 0.75 mm) [Tm]**	$\int B_{nom} \mathbf{d}l$ **[Tm]**	I_{nom} **[A]**
RCBX1	0.10	0.08	2.5	1600
RCBX2	0.10	0.08	2.5	1600
RCBX3	2.12	0.20	4.5	1600
RCBRD4	3.17	0.10	5	430
RCBY4	0.64	0.02	2.79	88

The 11 T magnets will be in series with the main dipoles circuits, so they need to sustain at least 10 A/s. An additional trim is foreseen to compensate for the different transfer function with respect to the nominal bending magnets. Figure 7 shows the needed trim current as a function of the main bending currents [26]. The minimum current is about -232 A when the beam energy is about 3.5 TeV, while for nominal operations at 7 TeV the trim current should be approximately zero. According to the present operational scenarios [27] the nominal HL-LHC beam energy will be 7 TeV, however, operation at intermediate energies could be possible, as it has been done in the LHC. This would require a constant trim current different from zero during stable beams. Assuming the nominal ramp rate for the main bends (10 A/s), and computing the numerical derivative of the function in Fig. 7 one obtains Fig. 8. From this the extreme trim ramp rates are -0.45 A/s and 0.55 A/s during the first and second half of the ramp, respectively.

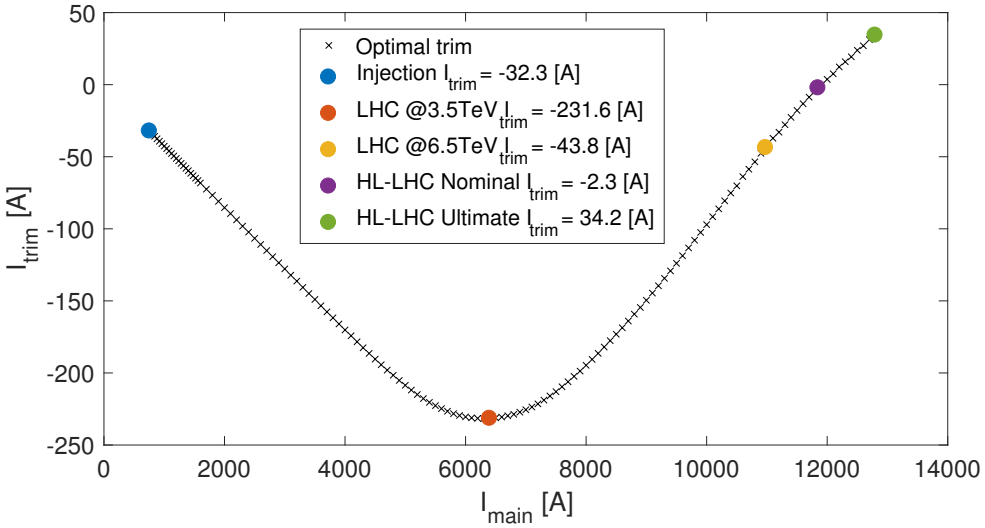

Fig. 7: Ideal 11 T dipole trim current as a function of the main dipole current [26]. The main working points (Injection, 3.5 TeV, 6.5 TeV, 7 TeV, 7.5 TeV) are highlighted by coloured dots.

Table 9 summarises, where applicable, the ramp rates for the different circuits as determined in this section. A first guess of acceleration rates is also derived following the scaling law of Eq. (8).

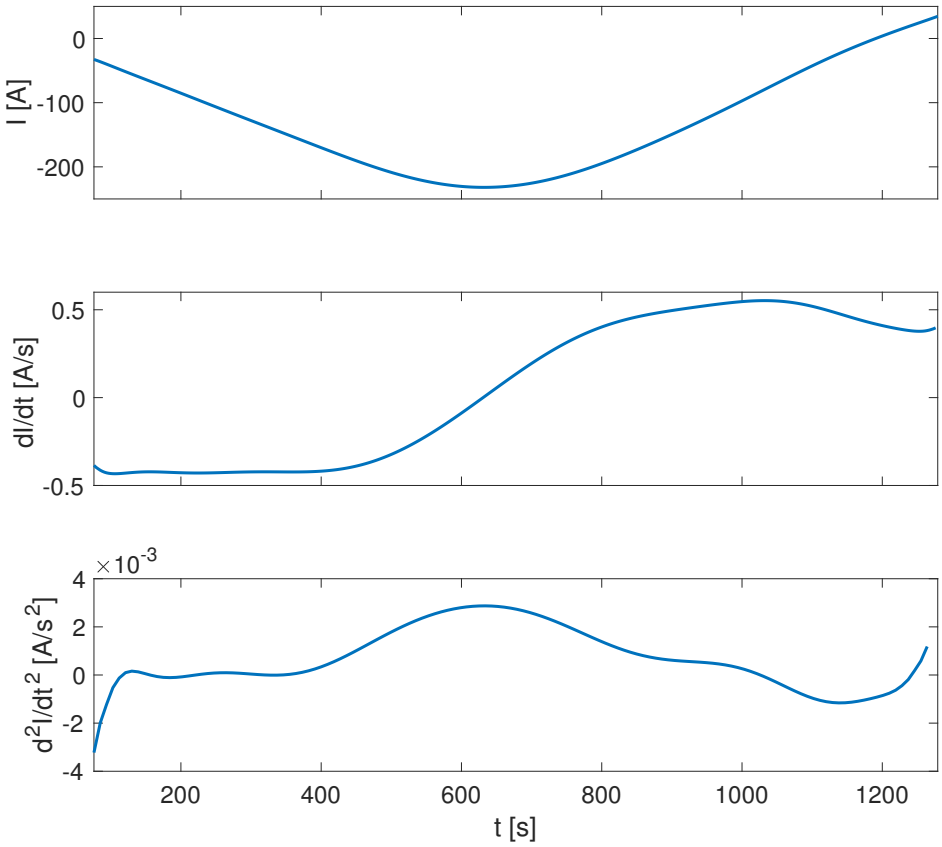

Fig. 8: Ideal 11 T dipole trim current and time derivatives as a function of time assuming constant 10 A/s ramp for the main dipole.

Table 9: Summary of nominal ramp rates for the new HL–LHC circuits resulting from energy ramp considerations. The values in parenthesis have to be considered as rough estimates.

Circuit	I_{nom}**[A]**	**Ramp rate [A/s]**
RQX	16470	13.90
RCBX	1600/1470	(0.64)
RD(1/2)	12000	10.13
RCBRD	430	(0.23)
RQ(4/5)	4510	(3.81)
RCBY	88	(0.02)
RQ6	4310	(3.64)
RTB8	250	0.55

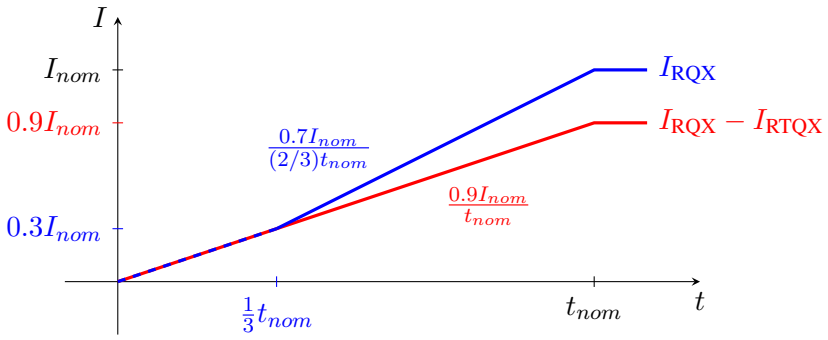

Fig. 9: Simplistic scheme (not to scale) of triplet main circuit currents during "ramp and squeeze".

3.2 Squeeze

The pre-squeeze or squeeze can only be performed when the beam size allows for increasing the β functions at the matching sections and in the arcs for the ATS optics. In the HL–LHC baseline of IR1 and IR5 the triplets and the matching section quadrupole strengths are modified during the so called pre-squeeze, which, in part, takes place during the ramp in the so called "ramp and squeeze" [1]. In the present operational scenario [27] The squeeze is performed at collision energy and it acts mainly on the matching section quadrupoles of the neighboring insertions.

Earlier studies showed that the pre-squeeze and squeeze in HL–LHC should take approximately 200 s if they are both performed at collision energy [28]. In the LHC it has been proven that the pre-squeeze can start already during the ramp (approximately at 2 TeV), as it is also visible in Fig. 1. Most of the matching section quadrupoles need to reduce their strength during the pre-squeeze. These quadrupoles benefit of a *temporary* reduction of their ramp rates during the "ramp and squeeze", but for other quadrupoles the effect is opposite. Moreover, the recent experience with the ATS optics in the LHC revealed that the ramp rates of the arc sextupoles and Landau octupoles might become a limiting factor [29] for "ramp and squeeze" in HL–LHC. In any case, at least part of the 200 s previously mentioned could be gained at collision energy.

An important point is that with "ramp and squeeze" the triplets might require a faster ramp rate. In preliminary pre-squeeze sequences the strength of Q2 needs to increase of about 3 to 4% [30] with respect to the other triplet quadrupoles, but this imbalance might reach 10% as allowed by the trim current range for possible new optics [1]. With the present circuit layout (see Appendix C) the ramp rate of Q2 will be equal to the ramp rate of the common RQX circuit, while the RTQX1 and RTQX3 trims will need to provide any additional ramp rates for Q1 and Q3. Based on the present experience, the pre-squeeze could start at about ⅓ of the energy ramp, as visible in Fig. 1. The simplest scenario assuming piecewise constant ramp rates that might well represent the worst scenario is depicted in Fig. 9. Here it is assumed that the whole triplet is ramped up by the main RQX circuit only during the first ⅓ of the energy ramp time (t_{nom}). Afterwards the main circuit needs to increase its speed to bring Q2 at the nominal current, while the trim circuits keep Q1 and Q3 strengths 10% lower than I_{nom} at the end of the ramp. At the beginning the required ramp rate for RQX is only 90% of what specified in the previous section, i.e. $0.9 \times 13.90 = 12.51$ A/s. Afterwards the same circuit needs to ramp up 70% of I_{nom} in ⅔ of the total ramp up time. This results in a required ramp rate of $0.7/(2/3) \times 13.90 = 14.60$ A/s. At the same time the trim circuits on Q1 and Q3 need to compensate for the extra current, i.e. they need to provide $12.51 - 14.60 = -2.09$ A/s. In the LHC the end of the ramp is performed in about 20 s. In order to decelerate from the full speeds computed above, $14.60/20 = 0.73$ A/s^2 and $2.09/20 = 0.11$ A/s^2 are needed for the RQX and RTQX circuits, respectively.

A limitation today in obtaining a faster pre-squeeze is the operational need of going through several "check-points" with zero derivative on the quadrupoles relative strength. This slows down the process

and induces voltage spikes that can be mis-interpreted as magnet quench by the QPS and therefore trigger unwanted beam dumps. A proposed solution would be to upgrade the squeeze implementation strategy with no check-points [30]. This would also allow to implement a faster ramp and squeeze. Figure 10 shows the current ramp rates for Q1, Q2 and Q3 resulting from a possible implementation of a ramp and squeeze starting from the middle of the ramp and able to arrive at the end of ramp with the nominal 64 cm β^* in IP1 and IP5 [27, 31]. Note that the maximum ramp rates for Q2 (< 15 A/s) as well as the

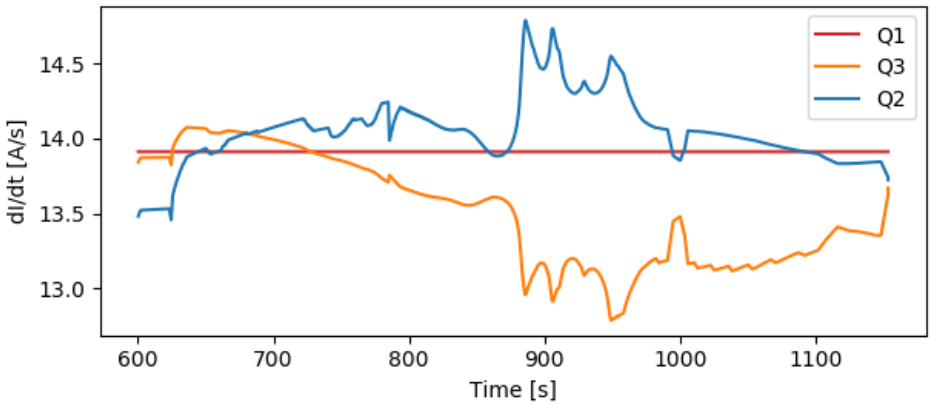

Fig. 10: Necessary current ramp rates for Q1, Q2 and Q3 as a function of time (in seconds from the start of the ramp) during a possible implementation of ramp and squeeze.

difference between Q2 and Q3 (< 2 A/s) are compatible with the simplified model previously used for the RQX and RTQX circuits. Still, it is important to allow for additional margin for possible optimisation of aperture, injection and pre-squeeze β^*, phase advance and crab cavity angle.

Currently no further specifications are provided for the ramp rates of matching section quadrupoles and optics correctors RQSX and RC(S/O/D/T)X related to the squeeze process. It is expected that the squeeze will not impose tighter constrains than the ones identified by other means in this document. In HL–LHC it is also foreseen to introduce β^* levelling. This process is very slow compared to the energy ramp and squeeze processes, therefore it is also assumed not to put constrains on the ramp rates.

Table 10 summarises the ramp rates for the different circuits as determined in this section.

Table 10: Summary of nominal ramp rates for the new HL–LHC circuits resulting from squeeze considerations.

Circuit	I_{nom}**[A]**	**Ramp rate [A/s]**	**Acceleration [A/s^2]**
RQX	16470	14.60	0.73
RTQX1	2000	2.09	0.11
RTQX3	2000	2.09	0.11

3.3 Ramp down time

From the analysis in Section 2.2.2 it was found that the LHC main bending magnets and arc quadrupoles ramp down from 6.5 TeV in about 1300 s. For the nominal 7 TeV operations one expects about 100 s more, i.e. 1400 s. The absolute minimum ramp-down time can be estimated assuming a constant ramp rate of -10 A/s for main dipoles, i.e. $11850/10 = 1185 \approx 1200$ s. It has to be stressed that the bottleneck will remain the ramp down time of IR2/8 triplets which are presently not planned to be upgraded in the

framework of HL–LHC. Those circuits will still limit the ramp-down time to approximately 2300 s if no action is taken. As presented in Section 2.2.2, the presently long ramp-down time is comfortably used for the degaussing cycles of the 600 A circuits and to bring the matching section quadrupoles to a predefined value before starting their discharge. Both operations could be reduced in length or skipped [10, 25]. It is therefore recommended to target about 1200 s for the ramp down time for all new HL–LHC magnets in order to maximise the opportunities for future turnaround reduction. However, in case an upgrade of the IR2/8 triplets will be planned, one will also need to optimise and verify the degaussing cycles of the 600 A circuits in order to evaluate the actual reduction of the turnaround [10].

The ramp down of circuits with 1 quadrant PCs is expected to follow the behaviour of a RL circuit:

$$I(t) = I_{nom} \exp\left(-\frac{t}{\tau}\right) \tag{10}$$

where τ is the time constant of the circuit which is defined as $\tau = L/R$ where R and L are the resistance and the inductance of the circuit, respectively. Ideally the ramp down should end when the current is approximately 200 A below the value required for the next beam injection [10, 25]. A reasonable assumption here is to reach 50% of the injection current. Assuming linear transfer function of the magnet strengths, one can define the length of the ramp down as:

$$t = -\ln\left(\frac{0.5 \times 450}{7000}\right)\tau = 3.44\tau \tag{11}$$

where 450 and 7000 are the injection and nominal beam energy, respectively. Assuming the previously defined ramp down time of 1200 s, the decay time of each circuit should be $\tau < 349$ s. As an alternative, one should foresee a two-quadrant PC.

3.4 Maximum ramp and acceleration rates

The energy ramp is not the most demanding process in terms of ramp and acceleration rates. Table 3 clearly shows that in the LHC the processes without beam (i.e. SETUP, BEAMDUMP, RAMPDOWN) exploit the maximum performance of most of the circuits. The very large negative speed reached by the main and matching section quadrupoles correspond to the beginning of their free-fall discharge during the RAMPDOWN. The maximum ramp and acceleration rates are instead exploited during the SETUP process and they are comparable with what specified in [4], and summarised in Table 1, for the LHC circuits powering tests. These values are the result of the experience matured with the LHC operation. For the new circuits a conservative approach could be to rescale the LHC ramp and acceleration rates of Table 1 with respect to the new nominal current of equivalent circuits in HL–LHC. For example, the LHC triplet main circuit (RQX) has I_{nom} = 6800 A and it is tested at 6.2 A/s and 1 A/s^2. In HL–LHC it will have I_{nom} = 16470 A, so one could target $6.2 \times 16470/6800 = 15.02$ A/s and $1 \times 16470/6800 = 2.42$ A/s^2. The same assumption can be applied to the other circuits, including the MQY quadrupoles which will increase their nominal current. All values obtained using this scaling law are reported in Table 11. Note that sometimes there is no direct correspondence between the new HL-LHC circuits and the current LHC circuits. The choice made in Table 11 is based on the similarity of the circuit function and nominal current.

Since this approach might result to be too conservative (e.g. for RCBX and RD(1/2)), the actual physical constrains imposed by other specific modes of operation are discussed in the following.

3.4.1 Optics measurement with K-modulation

In the LHC K-modulation is performed adding a sinusoidal excitation on Q1 or Q2. The amplitude and the frequency of the modulation depend on the actual optics and the required accuracy of the measurement [32]. Typical values for LHC are 5 A amplitude and 60 s period [29].

Table 11: Ramp rates for the new HL–LHC circuits obtained by scaling the performance of the equivalent (wherever applicable) LHC circuits as reported in Table 1.

HL–LHC circuit	**Equivalent LHC circuit**	I_{nom}**[A]**	**Ramp rate [A/s]**	**Acceleration [A/s^2]**
RQX	RQX (IR1, IR5)	16470	15.04	2.42
RTQX1	RTQX2 (IR1, IR5)	2000	1.74	0.37
RTQXA1	n.a.	35	n.a.	n.a.
RTQX3	RTQX2 (IR1, IR5)	2000	1.74	0.37
RCBX	RCBX	1600/1470	7.41	0.60
RQSX	RQSX	182	0.91	0.46
RC(S/O)X	RC(O/S/T)X	105	0.53	0.26
RC(D/T)X	RC(O/S/T)X	105	0.53	0.26
RD(1/2)	RD2 (IR1, IR5)	12000	33.33	5.14
RCBRD	RCBY(H/V)(4-5)	430	3.98	1.49
RQ(4/5)	RQ4 (IR1, IR5)	4510	13.53	2.50
RCBY	RCBY(H/V)(4-5)	88	0.82	0.31
RQ6	RQ6 (IR1, IR5)	4310	12.93	2
RCBC	RCBC(H/V)(5-6)	80	0.67	0.25
RTB8	n.a.	250	n.a.	n.a.

The tune variation ($\Delta Q_{x,y}$) as a function of the integrated quadrupole strength variation (ΔKL) is governed by the following Equation [33]:

$$\Delta Q_{x,y} \approx \pm \langle \beta_{x,y} \rangle \frac{\Delta KL}{4\pi} \tag{12}$$

where $\langle \beta_{x,y} \rangle$ are the average β functions at the quadrupole used for the modulation and $\pm$ sign refers to the horizontal and vertical planes, respectively. The integrated quadrupole strength KL is approximately equal to

$$KL \approx \frac{gL}{3.356p} \tag{13}$$

where g and L are the quadrupole field gradient in T/m and the magnetic length in metres, respectively, p is the beam momentum expressed in GeV/c. The gradient g can be expressed as a function of the actual quadrupole current I:

$$g = I \frac{g_{nom}}{I_{nom}} \tag{14}$$

where g_{nom} is the nominal gradient. One can therefore rewrite Eq. (12) as:

$$\Delta I \approx \pm 4\pi \frac{\Delta Q_{x,y}}{\langle \beta_{x,y} \rangle} \frac{I_{nom}}{g_{nom}} \frac{3.356p}{L} \tag{15}$$

that expresses the current variation ΔI to be applied on a specific quadrupole in order to introduce a tune variation ΔQ.

K-modulation is performed by applying a sinusoidal excitation of amplitude I_0 and period T:

$$I(t) = I_0 \sin(\frac{2\pi}{T} t). \tag{16}$$

Therefore, during the measurement the required circuit ramp and acceleration rates are:

$$\frac{\mathrm{d}I(t)}{\mathrm{d}t} = I_0 \frac{2\pi}{T} \cos(\frac{2\pi}{T}t); \qquad \frac{\mathrm{d}^2 I(t)}{\mathrm{d}t^2} = I_0 \left(\frac{2\pi}{T}\right)^2 \sin(\frac{2\pi}{T}t). \tag{17}$$

The tight requirements for β^* measurement precision in HL–LHC will require to induce a substantial tune shift by acting on the closest quadrupole to the IP. For β^* below or equal to 20 cm it turned out to be necessary to act only on Q1A and hence the request for a dedicated trim circuit on this magnet [34, 35]. The maximum tolerable tune shift in HL-LHC will be 0.01. This will be sufficient to meet the specification for the 20 cm β^* optics only, while for lower β^* (e.g. for the nominal 15 cm optics) new techniques for reducing the errors will need to be studied [35]. Note that the smaller the β^*, the higher is the β function at the triplets, hence a smaller excitation is needed for inducing the same tune shift of 0.01. It is therefore reasonable to consider the 20 cm optics and a tune shift of 0.01 as maximum requirements for k-modulation using the available circuits. Figure 11 shows the round collision optics in the region of IR5 triplets for Beam 1 (B1). The HL-LHC triplets have $g_{nom} = 132.6$ T/m and $I_{nom} = 16470$ A [1].

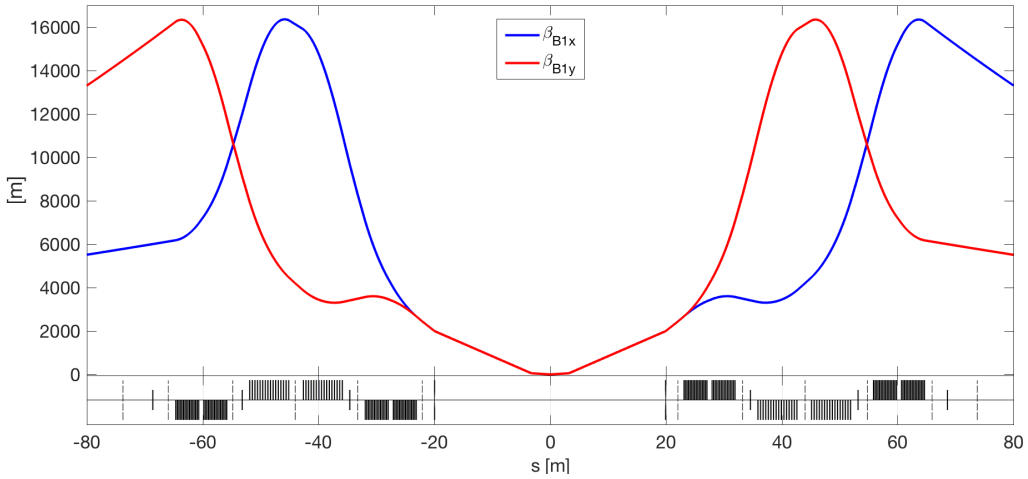

Fig. 11: Nominal Twiss β functions for B1 in the IR5 triplets region for 20 cm β^* round optics.

Table 12 reports the magnetic lengths of each triplet unit, the minimum of $\langle\beta_x\rangle$ and $\langle\beta_y\rangle$ for the nominal optics with 20 cm β^*, and the required circuit current variation needed to induce a 0.01 beam tune shift at 7 TeV according to Eq. (15) to the beam/plane with minimum beta function. The associated maximum ramp and acceleration rates involved during a 60 s period sinusoidal excitation are also reported.

Note that according to the present circuit baseline (see Appendix C) there will be the possibility to apply a trim current only to the full Q1, Q3, or to the single Q1A unit. An additional possibility is to excite Q2 by acting on the whole RQX circuit and by compensating with RTQX1 and RTQX3. Taken those considerations, the relevant specification from this section are summarised in Table 13.

3.4.2 11 T trim circuit

From the required trim current showed in Fig. 7 and the numerical differentiation presented in Fig. 8 one can see that during the energy ramp the maximum ramp rate is about 0.55 A/s and the maximum acceleration rate is less than 0.01 A/s^2. At the end of the energy ramp the main dipoles circuits quickly decelerate to reach the steady condition. A similar behaviour needs to be followed by the trim circuit. Since the main dipoles are expected to sustain 1 A/s^2 and a speed of 10 A/s (see Table 1), also the trim should be able to follow the same acceleration normalised by the ratio of the maximum speeds. This

Table 12: Magnetic length (L) [1], minimum average β function between the two transverse directions at IR5 triplets for round collision optics (20 cm β^*), and relative circuit current variation and ramp rates needed for 0.01 beam tune shift assuming a sinusoidal excitation of period of 60 s.

Quadrupole	L **[m]**	$\langle\beta_{min}\rangle$ **[m]**	**max** ΔI **[A]**	**max ramp rate [A/s]**	**max acc. rate [A/s^2]**
Q1A	4.20	3062	31.7	3.32	0.35
Q1B	4.20	3567	27.2	2.85	0.30
Q1A+Q1B	8.40	3315	14.6	1.53	0.16
Q2A	7.15	3458	16.5	1.73	0.18
Q2B	7.15	5890	9.7	1.01	0.11
Q2A+Q2B	14.30	4674	6.1	0.64	0.07
Q3A	4.20	8311	11.7	1.22	0.13
Q3B	4.20	6477	15.0	1.57	0.16
Q3A+Q3B	8.40	7394	6.6	0.69	0.07

Table 13: Summary of ramp rates for the new HL–LHC circuits resulting from K-modulation considerations.

Circuit	I_{nom}**[A]**	**Ramp rate [A/s]**	**Acceleration [A/s^2]**
RQX	16470	0.64	0.07
RTQX1	2000	1.53	0.16
RTQXA1	35	3.32	0.35
RTQX3	2000	0.69	0.07

Table 14: Summary of ramp rates for the 11 T trim circuit.

Circuit	I_{nom}**[A]**	**Ramp rate [A/s]**	**Acceleration [A/s^2]**
RTB8	250	1	0.1

gives $1 \times 0.55/10 \approx 0.06$A/s^2. Given these modest requirements for both ramp and acceleration rates, rounded specifications are proposed and reported in Table 14.

Note that, given these specifications, the 11 T magnet itself in the worst case will need to sustain the maximum ramp of the main bends plus the maximum ramp of the trim, i.e. 11 A/s and 1.1 A/s^2.

3.4.3 Orbit corrector circuits

The present inner triplet correctors cannot be used by the orbit feedback during LHC operations. Even though this is not a major issue for LHC, the installation of the crab cavities will introduce additional and tighter orbit constrains in HL–LHC in the region of IR1 and IR5. It is therefore required to allow the feedback for using the new MCBXF in HL–LHC.

A proposal for increasing the speed of the MCBXF correctors was presented in [1] and it is reported in Table 15. The equalisation applied is meant to ensure that all correctors will be able to kick the beam as fast as the existing MCBY correctors, which are presently compatible with the orbit feedback. The MCBY can provide about 0.91 μrad/s and 0.34 μrad/s^2. The new MCBXFB will be the weaker magnet in terms of integrated field for a higher nominal current with respect to the LHC equivalent MCBX. In order to reach 1 μrad/s and 0.33 μrad/s^2 the new PC and QPS will need to allow for 15 A/s and

5 A/s^2. The same argument is used for defining the ramp rates of the MCBRD. The MCBXFA is almost two times stronger than the MCBXFB for the same nominal current. Assuming that the MCBXFA and MCBXFB will use the same type of PC, the MCBXFA will be about 80% faster than the MCBXFB. The ramp rates for D1 and D2 specified in [1] were a first proposal which was obtained by scaling the

Table 15: Comparison of the relevant orbit correctors and separation dipoles [1].

	MCBXFA	**MCBXFB**	**MCBRD**	**MCBY**	**MBXF**	**MBRD**
Nom. Int. field [Tm]	4.50	2.50	5.00	2.79	35.00	35.00
Nom. Current [A]	1600	1600	430	88	12000	12000
Ramp rate [A/s]	15.00	15.00	2.00	0.67	12.00[a]	12.00[a]
Field Rate [mTm/s]	42.19	23.44	23.26	21.15	35.00	35.00
Angle Rate [μrad/s @ 7TeV]	1.81	1.00	1.00	0.91	1.50	1.50
Ramp Acc. [A/s^2]	5.00	5.00	1.00	0.25	2.00	2.00
Field Acc. [mTm/s^2]	14.06	7.81	11.63	7.93	5.83	5.83
Angle Acc. [μrad/s^2 @7TeV]	0.60	0.33	0.50	0.34	0.25	0.25
Time to nom. rate [s]	3.00	3.00	2.00	2.67	6.00	6.00

[a] In [1] it was specified 20 A/s as a first estimation.

performance of the present D2 (see Table 1) [31]. Presently the strategy is to use values from Table 9 with some margin, i.e. 12 A/s [36, 37]. This is largely enough to obtain kick speeds that are comparable with the nearby orbit correctors.

Another important constraint is the speed of the beam-beam separation collapse when going in collision. In order to avoid beam-beam driven instabilities one should cross the final phase from 2 to 0 σ in less than 3 seconds [38, 39]. In this phase one can assume to be in full deceleration of the collapse speed, so this translate in fulfilling the relation:

$$\frac{1}{2}a(3)^2 = 2\sigma \tag{18}$$

where a is the required acceleration rate in order to separate the beams by 2 σ in 3 s. This results in $a = 0.44\ \sigma/\mathrm{s}^2$. Assuming $\epsilon_n = 2.5\ \mu$m and the worst case $\beta^* = 70$ cm, then the ± 0.75 mm associated to the separation knob presented in Table 8 corresponds to

$$\frac{\pm 0.75}{\sqrt{0.7 \times 2.5 \times 0.938/7000}} \approx \pm 49\sigma. \tag{19}$$

From Table 8 the MCBXF3 (i.e. RCBX3 circuit) current needed for $\pm 1\sigma$ separation, i.e. 2 σ total separation, is

$$I_{nom}\frac{B_{sep.\ knob}}{B_{nom}}\frac{1}{49} = 1600 \times \frac{0.2}{4.5} \times \frac{1}{49} = 1.45\frac{\mathrm{A}}{\sigma}. \tag{20}$$

Combining the two previous relations one obtains an acceleration rate requirement of 0.64 A/s^2. By using the same relations one obtains 0.09 A/s^2 for the MCBRD4 (i.e. RCBRD circuit) and 0.01 A/s^2 for the MCBY4 (i.e. RCBY4 circuit).

The orbit correctors might also need to be cycled once up to $\pm I_{nom}$ during the RAMPDOWN as presently done by the 600 A circuits in the LHC. This translates in requiring a maximum ramp rate of $1600/(1200/4) = 5.33$ A/s, assuming to perform a triangular shape cycle within the target RAMPDOWN time of 1200 s length. A reasonable assumption for the acceleration rates is to be able to perform the ramp rate inversion in approximately 10 s, i.e. $2 \times 5.33/10 = 1.66$ A/s^2.

Note that all the requirements for orbit collapse and circuit cycle are well within the requirements reported in Table 15, and summarised in Table 16 with respect to the corresponding circuit names.

Table 16: Summary of ramp rates for the linear orbit corrector circuits.

Circuit	I_{nom}**[A]**	**Ramp rate [A/s]**	**Acceleration [A/s^2]**
RCBX	1600/1470	15	5
RD(1/2)	12000	12	2
RCBRD	430	2	1
RCBY	88	0.67	0.25

3.4.4 Non-linear corrector circuits

The main constraint for the non-linear correctors are the degaussing cycles these circuits might require before injecting the beam. The present strategy is to perform 4 triangular cycles: the first with amplitude up to $\pm I_{nom}$ and then progressively reduced by 25% of I_{nom} at each cycle [37]. The degaussing time needs to be shorter than the RAMPDOWN, i.e. less than 1200 s, therefore the maximum single cycle length has to be approximately 300 s. The most demanding cycle is the first one: its maximum ramp rate can be estimated as $4 \times I_{nom}/300$. For the order 2 correctors ($I_{nom} = 182$ A) this translate in 2.42 A/s, while for higher order correctors ($I_{nom} = 105$ A) it is 1.40 A/s. As for the orbit corrector, in order to perform the current inversion in approximately 10 s the circuits need $2 \times 2.42/10 = 0.48$ A/s^2 for the order 2 correctors and $2 \times 1.40/10 = 0.28$ A/s^2 for the higher order correctors. Note that this requirement might be relaxed if the remanent field will be found to be low enough not to require degaussing cycles. Magnetic measurements are foreseen in 2017 [37].

An additional constraint could come in case of K-modulation-based measurement of the beam offset at the location of these magnets. However, a strategy for such a measurement has not been defined yet [29] and so no requirements are defined here also because this is expected to be in the shadow of the degaussing requirements.

The relevant specifications from this section are summarised in Table 17.

Table 17: Summary of ramp rates for the new HL–LHC non-linear corrector circuits resulting from degaussing cycles.

Circuit	I_{nom}**[A]**	**Ramp rate [A/s]**	**Acceleration [A/s^2]**
RQSX	182	2.42	0.48
RC(S/O)X	105	1.40	0.28
RC(D/T)X	105	1.40	0.28

3.5 Precycle

In the LHC it is foreseen to perform a precycle whenever is needed to ensure a reproducible behaviour of the magnets. From the LHC experience the precycle consists in ramping triplets, main quadrupoles and main dipoles approximately up to half the nominal current (i.e. equivalent to 3.5 TeV) [40], keep this flattop for 10 minutes and finally ramp down below the current required for the injection, as it is done for the normal ramp down. The cold separation dipoles (D1 and D2) and the matching section quadrupoles are brought to a predefined current equal to or slightly below I_{nom}. These magnets are kept at flattop for a minimum of 300 s before being discharged again below the injection current. At the same time most

of the other circuits are cycled with a single oscillation of amplitude equal to $\pm I_{nom}$, while the Landau octupole magnets are degaussed with three (originally four) full cycles of decreasing amplitude [10, 41].

All new circuits should be compatible with the above strategy without increasing the length of the precycle (which presently last about 40 minutes [40]). A conservative limit for the maximum allowed time is the minimum duration of the main dipoles precycle. Given the nominal current and ramp rates in Table 1, this time is approximately 1800 s (600 s for each ramp and 600 s at flattop). The cycles for the new linear and higher order corrector have been already specified in the previous sections to be within the 1200 s of the RAMPDOWN. Also the triplet circuits, since they will be powered by 2 quadrant power supply, will be able to follow the cycle of the main bending magnets. The only concern is therefore the precycle of D1/D2 and matching section quadrupoles that are foreseen to have 1 quadrant PCs [42]. They will need to be ramped up to $\approx I_{nom}$, kept at flat top for 300 s [10] and then discharged in free fall. The discharge decay time from I_{nom} is governed by Eq. (11), i.e. $t = 3.44\tau$. According to the present estimate of circuits resistance and inductance [42], the worst decay constants τ are 107 s for D2, and 123 s for Q5, therefore the total time needed for the ramp down is 368 s for D2 and 424 s for Q5. Considering the requirement of 300 s flat top and the target cycle time of 1800 s, the D2 circuit needs to ramp up in $1800 - 300 - 368 = 1132$ s, while Q5 in 1076 s. Assuming a simple linear ramp, the ramp rates required are $12000/1132 = 10.60$ A/s for D2 and $4510/1076 = 4.19$ A/s for Q5. Those values are reported in the summary Table 18.

Table 18: Summary of ramp rates for the new HL–LHC circuits resulting from considerations on the precycle length.

Circuit	I_{nom}**[A]**	**Ramp rate [A/s]**
RD(1/2)	12000	10.60
RQ(4/5)	4510	4.19

An alternative approach for the calculation is to consider the maximum ramp rates presently assumed in [3] for the ramp up to I_{nom}, and then compute the allowed ramp-down time to fit within the proposed 1800 s, i.e.:

$$\tau = \frac{1800 - 300 - I_{nom}/\left(\text{assumed max. ramp rate}\right)}{3.44}. \tag{21}$$

The assumed ramp rates and the resulting discharge maximum time constants (τ) resulting from Eq. (21) are summarised in Table 19.

Table 19: Maximum allowed circuit decay time constant to allow for 1800 s-long precycle given the ramp rates assumed in [3].

Circuit	I_{nom}**[A]**	**Assumed max. ramp rate [A/s]**	**Min. ramp-up time [s]**	**Max.** τ **[s]**
RD(1/2)	12000	12	1000	145
RQ(4/5)	4510	11	410	316
RQ6	4310	13	332	340

Also note that some circuits might require a different pre-cycle in HL-LHC, e.g. it is expected to power the Landau octupole magnets since the injection, so their degaussing procedure might become less critical than in the LHC. Therefore, the final precycle policy might be reviewed by the FiDeL [43] Working Group.

3.6 Summary

The operational requirements for all new circuits in HL–LHC are summarised in Table 20. The values reported under the "MCF" column are those presently specified in [3]. The "Spec." values have been identified within this document at the tables referenced under the "Ref." column. All values identified in this document and reported in Table 20 are below or equal to the values presently specified in [3]. Note that the MQY and MCBY magnets will increase their nominal current due to the lower operating

Table 20: Summary of ramp and acceleration rates for the HL–LHC circuits quoted in [3].

Circuit	I_{nom}**[A]**	**Ramp rate [A/s]**		**Acceleration [A/s^2]**		**Ref.**
		Spec.	**MCF**	**Spec.**	**MCF**	
RQX	16470	14.60[a]	16	0.73[a]	2.5	Tab. 10
RTQX1	2000	2.09	2.1	0.16[a]	0.4	Tab. 10, 13
RTQXA1	35	3.32	4	0.35	0.4	Tab. 13
RTQX3	2000	2.09	2.1	0.11[a]	0.4	Tab. 10
RCBX	1600/1470	15	15	5	5	Tab. 16
RQSX	182	2.42	4	0.48	1	Tab. 17
RC(S/O)X	105	1.40	3	0.28	1	Tab. 17
RC(D/T)X	105	1.40	3	0.28	0.4	Tab. 17
RD(1/2)	12000	12[a]	12	2[a]	2	Tab. 16
RCBRD	430	2[a]	2	1[a]	1	Tab. 16
RQ(4/5)	4510	10.83[a]	11	2[a]	2	Tab. 1
RCBY	88	0.67[a]	0.67	0.25[a]	0.25	Tab. 16
RQ6	4310	12.93	13	2	2	Tab. 1
RCBC	80	0.67	0.67	0.25	0.25	Tab. 16
RTB8	250	1	1	0.1	0.1	Tab. 14

[a] Smaller value than what calculated in Table 11 using simple scaling law.

temperature. Assuming that the PCs for those magnets will not be upgraded, the values for ramp and acceleration rates from Table 1 are maintained. This should not have any relevant impact on ramp up and ramp down times.

The requirements in Table 20 allow for the ramp-up time of each circuit within 1200 s. The ramp-down time of circuits powered by 2 or 4 quadrant PCs is assumed to be the same as the ramp-up time. For all other circuits the general requirement is to have a decay time $\tau < 349$ s in order to ramp down in less than 1200 s. For the precycle of D1, D2 and matching section quadrupoles the decay time specification could be tighter depending on the maximum circuit ramp rates and on the actual inductance/resistance of the circuits. The present estimates of inductance/resistance available in [3] and the ramp rates specified in Table 20 are compatible with a precycle length of 1800 s (See Section 3.5).

Several "Spec." requirements reported in Table 20 are lower than what calculated in Table 11 using a simple scaling low with respect to the present LHC circuit performances. This underlines that the actual ramp and acceleration rates are the result of operational aspect which might not be strictly connected with the needs for regular physics run. It is therefore recommended to take enough margin to allow for unforeseen manipulations.

To be also pointed out that the 11 T dipole (MBH) as well as the Q1 and Q3 quadrupoles (MQXFA) will need to sustain the sum of main circuit and relative trims ramp and acceleration rates.

4 Uncertainty requirements for the new power converters of HL–LHC

The PCs ripple has two main implications: it can perturb the precision of the tune measurement, which is the primary method for measuring β^* by means of K-modulation, and it can impact the lifetime of the beam. The present document is an update with respect to what was already analysed and presented in [1].

In order to estimate the variation of the magnetic field ($\mathrm{d}B$) as a function of a modulation frequency (f), the following model has been used in Chapter 2 of [1]:

$$\mathrm{d}B(f) = \begin{cases} T_{Vacuum}(f) \times T_{ItoB}(f) \times \mathrm{d}I(f) & \text{for } f \leq f_0 \\ T_{Vacuum}(f) \times T_{ItoB}(f) \times T_{VtoI,load}(f) \times \mathrm{d}V(f) & \text{for } f > f_0 \end{cases} \tag{22}$$

where $\mathrm{d}I(f)$ and $\mathrm{d}V(f)$ are the current and voltage modulation of a PC respectively, $T_{VtoI,load}(f)$ is the response of the circuit from voltage to current, modelled by a RL circuit, $T_{ItoB}(f)$ is the transfer function of the magnet, $T_{Vacuum}(f)$ is the transfer function of the cold bore, absorber, etc. The choice of the limit frequency f_0 that separates the current-control regime ($f < f_0$) from the voltage-control regime ($f > f_0$) is a parameter of the power converter that can be chosen in the range from hundred mHz to about one Hz. This choice has an impact on the PC "drift during a fill" and "short term stability" performances introduced in Section 2.3. Presently it is assumed that $f_0 = 0.1$ Hz is a reasonable value for all new PCs.

A refined model with respect to Eq. (22) was presented in [44]:

$$\frac{\mathrm{d}B(f)}{B_{nom}} = \begin{cases} \frac{\mathrm{d}I(f)}{I_{nom}} & \text{for } f \leq f_0 \\ T_{Vacuum}(f) \times T_{VtoB}(f) & \text{for } f > f_0 \end{cases} \tag{23}$$

$$\text{with: } T_{VtoB}(f) = T''_{VtoB}(f) \times \frac{\mathrm{d}V(f)}{2\pi f L_{DC} I_{nom}} \tag{24}$$

where L_{DC} and I_{nom} are the apparent inductance and the nominal current of the circuit respectively, B_{nom} is the nominal magnetic field imposed to the beam, while $T''_{VtoB}(f)$ is a correction term that can be ideally set to 1 in the cases where the frequency dependence ($T_{VtoB}(f)$) is well modelled by the expression that follows in Eq. (24). Experimental measurements of $T_{VtoB}(f)$ and $T_{Vacuum}(f)$ are foreseen in SM18 [44], while a detailed study on $T_{Vacuum}(f)$ is available in [45]. This will allow a better a more precise estimate of the actual *magnetic field* ripple seen by the beam starting from the PC performances.

Given the model in Eq. (23), one can assume that the current-control regime is fully described by the "stability during a fill (12 h)" and "Short term stability (20 min)" performance of the PC, as the transfer function between the variation of circuit current and magnetic field seen by the beam can be approximated to be equal to one. In the voltage-control regime one should take into account the additional terms $T_{Vacuum}(f)$ and $T_{VtoB}(f)$, which are normally smaller than one and rapidly decreasing for high frequencies.

All classes of PCs assumed to be available for HL-LHC are reported in Table 6.

Physics arguments are given in the following sections to constrain the choice of the new HL-LHC PC classes.

4.1 Tune measurement precision

In order to ensure a luminosity imbalance lower than 5% between IP1 and IP5 one needs better than 2.5% precision for β^* measurements [32]. Currently, the most precise method for β^* measurement is by using K-modulation. This technique relies on measuring beam tune variations while varying the strength of a set of quadrupoles and so it is limited by the natural noise on the tune. For such a measurement one

can assume to be dominated by the current-regime ripple of the PCs and in particular by the "short term stability (20 min)".

Earlier simulations showed that, assuming 0.1 ppm r.m.s. jitter on the new triplets PCs and 10^{-3} transfer function error and 5 mm r.m.s. longitudinal misalignment of the triplet quadrupoles, by applying K-modulation on Q2A one could obtain about 4% error on the β^* measurement, which would not be enough to reach the target luminosity imbalance [46]. For this reason, improvement of the β^* measurement technique have been studied and the introduction of the Q1A trim has been proposed in [46] and it is currently assumed as baseline, even though the details of its implementation are not known to-date. This could allow for reaching the required specification of 2 % at least for round beam (15 cm β^*) [46].

New simulations to verify the impact of the performance of the different circuits have been presented in [47]. Figure 12 shows the impact on tune variation per one ppm of I_{rated} of each relevant circuit in LHC and HL-LHC[4]. In the LHC the contribution of each arc main bending circuit (RB), due to the feed-down of the main sextupoles, is of the same order as the effect induced by the main triplet circuit (RQX) or by the trim on Q2 (RTQX2). The effect of the main quadrupoles is about half the main bendings one. Also Q4 has a noticeable impact, while Q5 and Q6 are much less prominent. The HL–LHC optics and any LHC ATS optics with similar telescopic index is about three times more sensitive to the strength variation of main triplet and some of the main bending circuits. This is expected due to the increased β function in the triplets and in the arcs participating to the telescopic squeeze.

A first analysis of measured tune stability for a few LHC optics is reported in Table 21. For each optics an estimation of the expected tune stability is also reported. The simulated values are computed by summing in quadrature the contributions to tune (Fig. 12a) times the assumed "short term stability (20 min)" of each circuit (Tables 6 and 7). The measured values are compatible with the simulations, despite the tested ATS optics (25 and 30 cm β^*) seem to provide a better tune stability than the nominal LHC optics. Dedicated measurements are foreseen to enrich the statistics.

Table 21: Tune jitter measured by means of AC-dipole kicks in LHC for different optics [47]. Simulated values are also reported for each optics. All measurements, except the 40 cm β^* non-ATS, have been performed in 2017.

	Tune jitter [10^{-5} r.m.s.]				
	40 cm β^* non-ATS	**40 cm β^* ATS**	**30 cm β^*; ATS**	**25 cm β^*; ATS**	**Ballistic**
Beam 1 (x)	5 ± 2	6 ± 2	0 ± 32	3 ± 2	0.9 ± 0.4
Beam 2 (x)	4 ± 2	4 ± 2	3 ± 2	1.7 ± 0.8	0.8 ± 0.4
Beam 1 (y)	2.4 ± 1.0	3.0 ± 1.2	1.7 ± 0.8	4 ± 2	0 ± 0.8
Beam 2 (y)	8 ± 4	0 ± 20	2.1 ± 1.1	2.6 ± 1.3	1.7 ± 0.7
Average	3.8 ± 1.5	3.9 ± 1.7	2.1 ± 1.0	2.6 ± 1.1	0.8 ± 0.4
Sim. Beam 1 (x)	1.85	1.82	2.22	3.07	1.04
Sim. Beam 1 (y)	1.83	1.81	2.22	3.01	1.01

4.2 Orbit stability

Figure 13 shows the impact on closed orbit of one ppm error on the relevant HL-LHC circuits. The values are normalised with respect to the local beam size assuming 7 TeV operation and 2.5 μm normalised emittance and 1.08×10^{-4} energy spread. Note that the most sensitive devices are the separation dipoles D1 and D2. Their impact on the orbit is higher than the impact of the triplets[5]. The perturbation induced

[4]It is assumed that the effect of P5 circuits is of the same order as for P1.

[5]The effect on orbit triggered by an error on the triplet is generated by the crossing scheme.

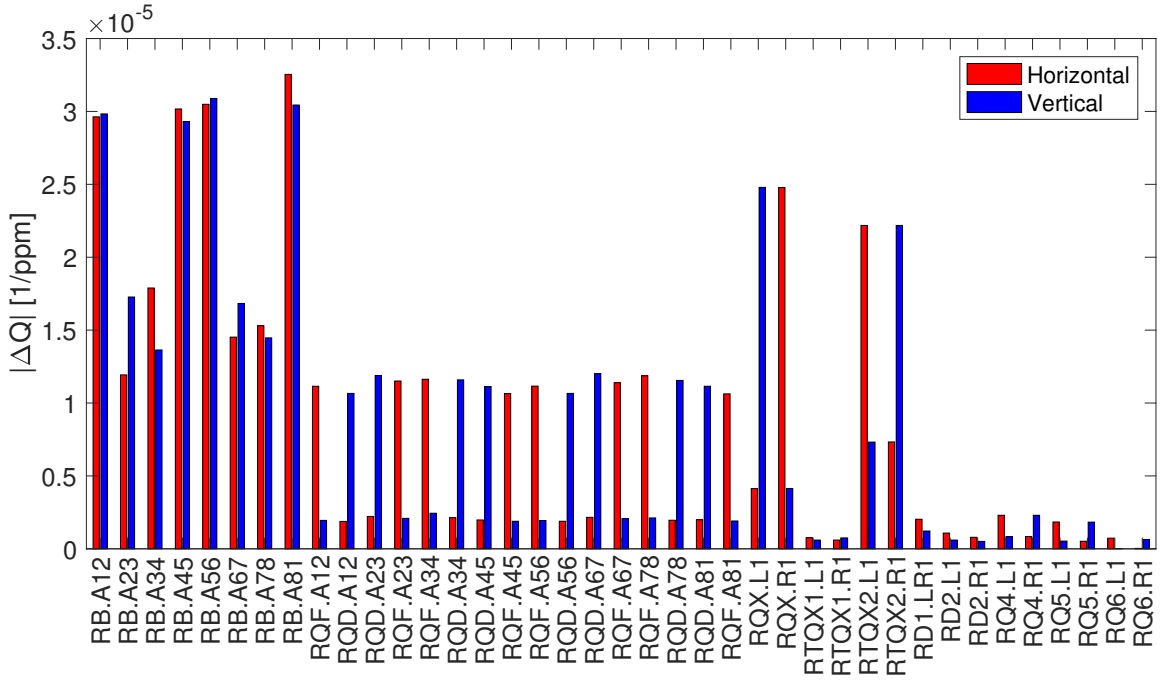

(a)

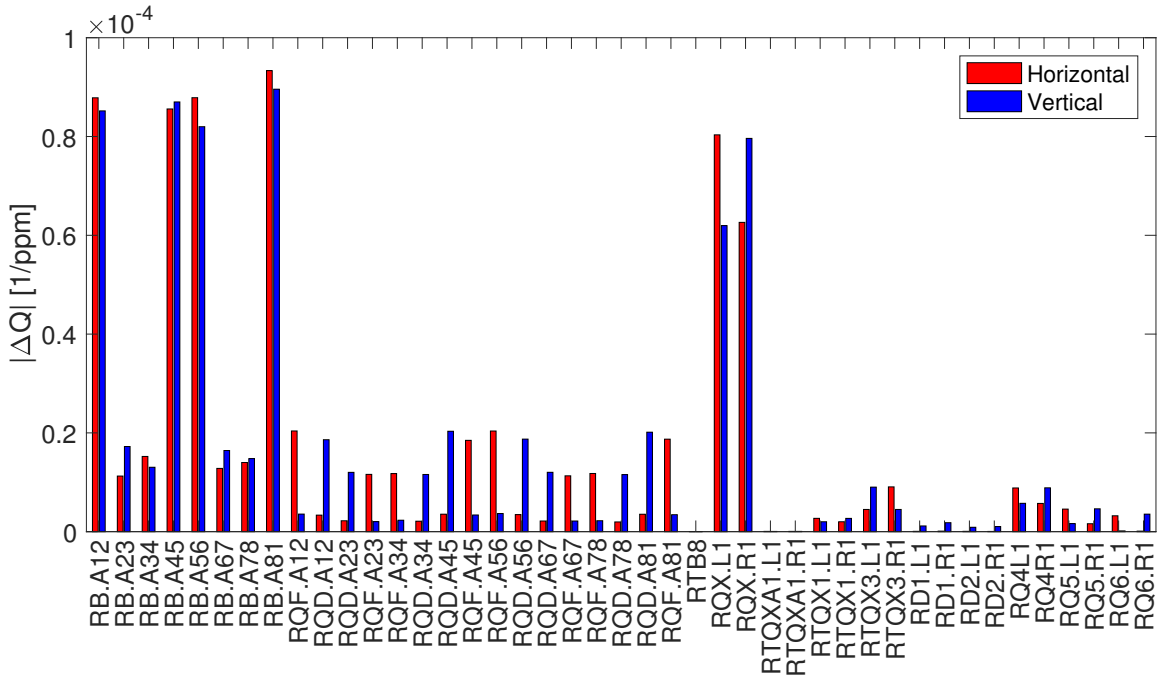

(b)

Fig. 12: Variation of Beam 1 tune per ppm of current variation (with respect to I_{rated}) for each of the main circuits of LHC with nominal 40 cm β^* round optics (a) and for HL-LHC with nominal 15 cm β^* round optics (b). The difference in between RB circuits for HL–LHC is due to the features of the ATS optics.

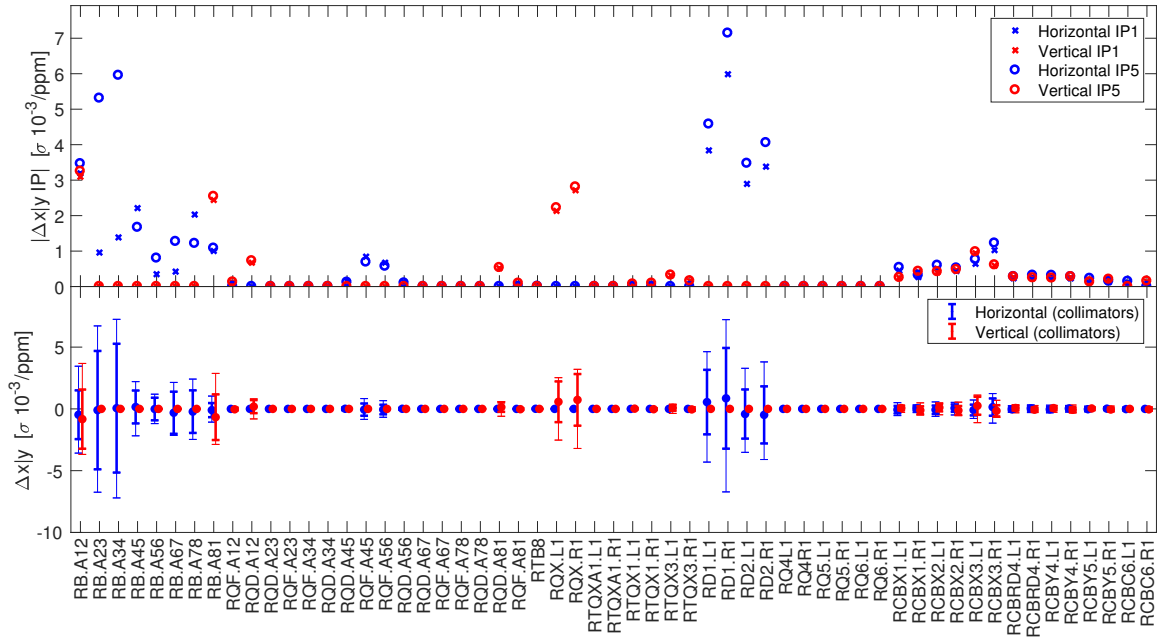

Fig. 13: Beam 1 orbit variation at IP1 and IP5 (top) and at the primary collimators (bottom) under the effect of one ppm error on each relevant circuit of HL-LHC with nominal 15 cm β^* round optics (HLLHCV1.3). In the bottom graph the thicker error bars give the mean and r.m.s. values, while the thinner error bars indicate the maximum excursion over all primary and secondary collimators. All values are normalised with respect to the local beam size.

by the other orbit correctors in the IR is about about 5 to 10 times smaller, while the impact of the 11 T dipoles trim (RTB8) seems to be negligible. Note that the impact of the main bend and of some main quadrupole PCs is also significant. Still, all contribution seems to be below one percent of beam sigma both at the IPs and at collimators.

During LHC operations it was observed an IP orbit stability during a fill of about half a beam sigma [48]. It is therefore expected that the PCs slow uncertainties have a negligible impact on orbit stability with respect, for example, to ground motion. For frequencies above a few tenths of Hz the orbit stability might play an important role due to beam-beam effects. Dedicated studies will need to be made to quantify those effects. For the time being, it is recommended to adopt the same class of PC for RQX and RD circuits. Also note that the expected inductance of the RD1 and RD2 circuits is approximately one order of magnitude lower that the RQX circuits [3], therefore, according to Eq. (24), the RD1 and RD2 circuits will be about 10 times more sensitive to PC voltage ripple than the RQX circuits.

4.3 Beta beating

Figure 14 shows the impact of one ppm error for the main HL-LHC circuits on beta beating at IP1 and IP5 and along the whole machine for the 15 cm β^* optics. The behaviour, as expected, reflects the impact on tune shown in Fig. 12b, and the main contributors are the main dipole of the ATS arcs and the main triplet circuit PCs. The amplitude of each contribution (less than 6×10^{-4} beta beating per ppm) together with the typically small "stability during a fill" values of the PCs (a few ppm, see Table 6) suggests a negligible impact on luminosity imbalance between IP1 and IP5 during a fill. However, this can become relevant on a longer time scale due to the drift accumulated by the PCs, i.e. due to their "long term fill-to-fill stability" uncertainty. Note that the impact of "initial uncertainty after calibration" and "linearity" uncertainties are eliminated, by definition, during the optics commissioning, as it is typically done at the beginning of year in the LHC.

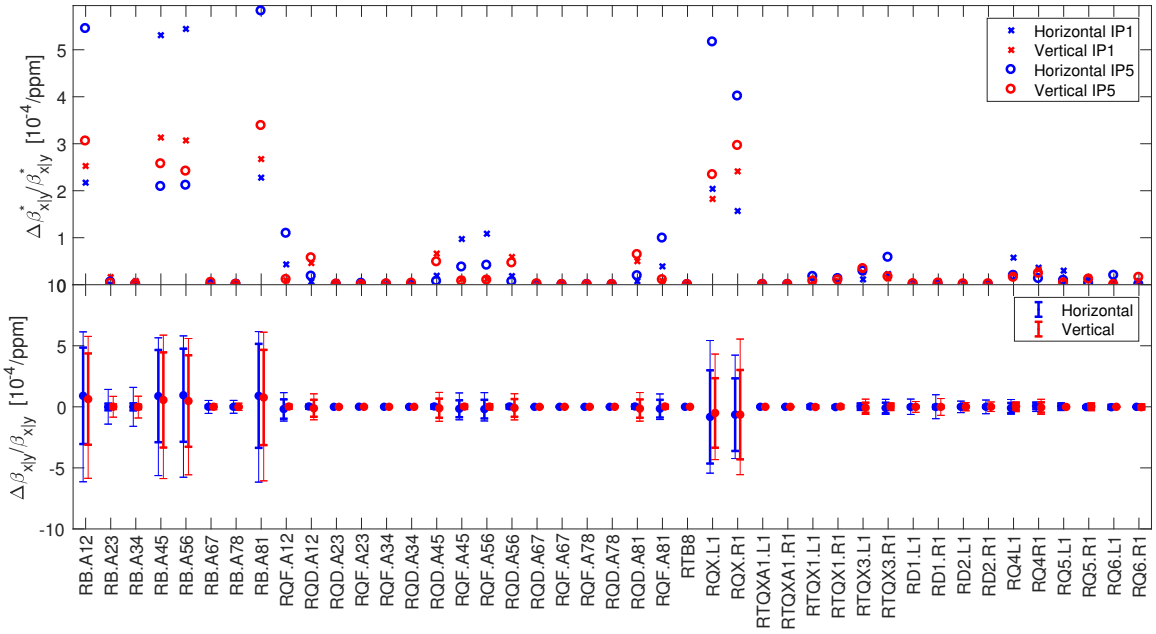

Fig. 14: Beam 1 beta beating at IP1 and IP5 (top) and at along the whole machine under the effect of one ppm error on each relevant circuit of HL-LHC with nominal 15 cm β^* round optics (HLLHCV1.3). In the bottom graph the thicker error bars give the mean and r.m.s. values, while the thinner error bars indicate the maximum excursion.

4.4 Proposed class for the new PCs

Based on the observations above, especially regarding K-modulation, the proposed PC classes for each HL-LHC circuit are provided in Table 22. For completeness, also the main bending and main quadrupole circuits are reported, as well as the corresponding "short term stability (20 min)" of each circuit. The power converters of the arcs and matching sections are assumed not to be upgraded. Table 23 shows the expected tune stability in HL-LHC for the nominal collision optics (15 cm β^*) and for different scenarios based on the propose HL-LHC PC class of Table 22. The column marked as "best" assumes to have zero uncertainty on all new PC , while "proposed" assumes the values reported in Table 22. For both cases the calculation has been repeated assuming to upgrade from class 1 to class 0 the main dipole PCs of the four ATS arcs (i.e. A12, A45, A56, A81). Note that the improvement on tune stability for such an upgrade is more than 30%, while the difference between "proposed" and "best" values is less than 10%.

Earlier studies showed that it would be desirable to keep the tune uncertainty below 10^{-5} in order to minimise the luminosity imbalance [46]. Unfortunately both simulations and measurements are presently exceeding this limit, therefore studies for improving the K-modulation technique are ongoing. More detailed informations are available in [35]. From the hardware side, a clear improvement could be achieved by upgrading the PC class of the main dipole PCs of the four ATS arcs.

From the orbit perspective, Table 24 summarises the expected orbit stability at IP1, IP5 and at collimators assuming the proposed PC classes. Note that also over a typical fill length the orbit stability due to the power converter stability seems to be in the shadow of what typically observed during operation (of the order of 50% of σ_{beam} at the IPs) and which is probably driven by magnet displacements due to ground motion [48]. Moreover, the suggested upgrade of some of the main dipole PCs would give a negligible improvement.

On the longer time scale, one can compute the maximum orbit and beta-beating drift that the machine could accumulate over one year, i.e. assuming the "long term fill-to-fill stability" performance

Table 22: Proposal of PC class (see Table 6) for the new HL-LHC circuits.

Circuit name	I_{rated} **[A]**	**PC class**	**short term stability [ppm** $2\times$**r.m.s.]**
RB[a]	13000	1	0.4
RQ(D/F)[a]	13000	1	0.4
RQX	18000	0	0.2
RTQX1	2000	2	1
RTQXA1	120[b]	4	5
RTQX3	2000	2	1
RCBX	2000	2	1
RQSX	200	3	2
RC(S/O)X	120	3	2
RC(D/T)X	120	3	2
RD(1/2)	13000	0	0.2
RCBRD	600	3	2
RQ(4/5)[a]	6000	2	1
RCBY[a]	120	4	5
RQ6[a]	6000	2	1
RCBC[a]	120	4	5
RTB8	300[c]	3	2

[a] Existing circuit assumed not to be upgraded.

[b] The rated current for this circuit has not been defined yet. The proposed value is compatible with the use of the trim.

[c] A standard 600 A PC of class 3 could also be adopted.

Table 23: Simulated HL-LHC tune stability (15 cm β^* optics HLLHCV1.3) assuming zero uncertainty on the new HL-LHC PC (best) or the class proposed in Table 22 (proposed).

	Tune jitter [10^{-5} **r.m.s.]**			
	best	**best***	**proposed**	**proposed***
Beam 1 (x)	3.80	2.24	4.13	2.77
Beam 1 (y)	3.72	2.22	4.05	2.75
Target			< 1	

* Assuming to also upgrade the PC of main bends in the ATS arcs to class 0.

of each PC. The worst case scenario can be computed by the sum in absolute value of all contributions presented in Fig. 13 and 14, respectively for orbit and IP beta beating, weighted by the corresponding "long term fill-to-fill stability" performance from Table 6. The values obtained are reported in Table 25. Note that this is a very pessimistic scenario, corresponding to all PC drifting of the maximum amplitude and in the worst configuration. The implementation and use of a remote controlled calibration system for the main triplet PCs and D1/D2, as existing for the main dipole and quadrupole PCs, could be beneficial for obtaining better luminosity stability over the year, however the continuous use of the orbit feedback and the introduction of luminosity levelling in HL-LHC might put those drift in the shade. Moreover, if a luminosity imbalance between IP1 and IP5 becomes observable along the year, it will be possible to perform either a dedicated calibration of the relevant PCs[6] during an HL-LHC Technical Stop (TS), or

[6]This is possible also for PCs not equipment with a remote controlled calibration unit. In this case one needs about half a

Table 24: Expected HL-LHC beam 1 orbit stability at IP1/5 and collimators for 15 cm β^* optics (HLLHCV1.3) on a short time scale (i.e. assuming the "short term stability (20 min)") and on a longer time scale (i.e. assuming "fill-to-fill repeatability"). The values are normalised with respect to the local beam size assuming 7 TeV operation and 2.5 μm normalised emittance and 1.08×10^{-4} energy spread. In parenthesis the values assuming to also upgrade the PC of main bends in the ATS arcs to class 0.

	Orbit jitter [10^{-3} $\sigma_{\textbf{beam}}$ **r.m.s.]**	
	Short time scale	Long time scale
IP1/5 (x)	2.9 (2.8)	6.5 (6.2)
IP1/5 (y)	2.2 (2.1)	4.7 (4.3)
Collimators (x)	2.2 (2.2)	5.2 (5.1)
Collimators (y)	1.7 (1.6)	3.5 (3.3)

Table 25: Worst HL-LHC beam 1 orbit and beta beating drift at IP1/5 for 15 cm β^* optics (HLLHCV1.3) on a year time scale (i.e. assuming the "long term fill-to-fill stability"). The orbit values are normalised with respect to the local beam size assuming 7 TeV operation and 2.5 μm normalised emittance and 1.08×10^{-4} energy spread. In parenthesis are the values obtained assuming a factor 2 improvement on main dipole and quadrupole PCs as well as on D1/D2 and main triplet PCs, corresponding to performing a calibration of those PCs every 6 months.

	Max |orbit drift| [$\sigma_{\textbf{beam}}$]	**Max** $\lvert\Delta\beta^*/\beta_0^*\rvert$
IP1/5 (x)	0.9 (0.7)	0.04 (0.02)
IP1/5 (y)	0.6 (0.5)	0.03 (0.02)

an additional optics measurement and correction.

4.5 Dynamic aperture perturbation

The main concerns for Dynamic Aperture (DA) are the high-frequency voltage tones. The voltage spectrum tones assumed in [1], Chapter 2.3.2, are reported in Table 26. Those values are also compatible

Table 26: Main PC voltage spectrum tones assumed in [1, 49].

Frequency	Amplitude [mV] r.m.s.
50 Hz	3.2
100 Hz	0.8
300 Hz, 20 kHz	10
600 Hz, 40 kHz	2.5
10 MHz	1
others	0.5

with the CERN custom acceptance levels (see Fig. 6) and no updated values are available, yet.

The previous DA simulations did not show major issues, but a factor 10 reduction of the ripple amplitude at 300 Hz was recommended [1]. To be noted that these simulations were assuming $T_{Vacuum}(f)$ equal to 1 and constant $T_{ItoB}(f)$ as a most pessimistic case. Ongoing measurements and simulations are

day per PC.

trying to give a more realistic estimation of the effect of the beam screen on $T_{Vacuum}(f)$ [44]. Preliminary results show a -3 dB cutoff frequency between 15 and 70 Hz followed by a fast decay with slope of at least -20 dB per decade [45]. If confirmed, this in itself could mitigate the concern about the 300 Hz ripple component. A final verification with the most recent optics and parametrisation is envisaged.

4.6 Tracking

Following the experience in [22], one can assume that during the energy ramp of the LHC the tracking error is dominated by the timing synchronisation between different circuits (better than 1 ms) and the "short term stability (20 min)" of the PCs. An element of novelty in HL-LHC, based on the latest LHC developments in Run2, is the introduction of the "ramp and squeeze". If for the LHC the main concern was the delay error between main dipoles and main quadrupoles, with "ramp and squeeze" also the error between circuits taking part in the squeeze might translate in undesired beta-beating or orbit excursion. Given the achievable delay error (here assumed to be < 1 ms) and by assuming the maximum ramp rate of each circuit, one can compute the equivalent circuit current error as:

$$\text{Induced current error} = (\text{delay error}) \times \frac{(\text{max ramp rate})}{I_{rated}}. \tag{25}$$

Table 27 summarises the resulting values for each circuit, to be compared to the "short term stability (20 min)" also reported. The assumed ramp rates come from Table 20 and the PC rated currents are those specified in [3]. Note that such an error has to be considered static, i.e. reproducible and so a-priori correctable. The dynamic error due to time jitter is negligible since the time jitter is expected to be of the order of a few μs.

Table 27: Expected induced current error by 1 ms static delay error at maximum ramp rate for the different HL-LHC circuits relevant to the discussion.

Circuit	I_{rated}**[A]**	**Ramp rate [A/s]**	**Delay-induced error [|.| max ppm]**	**Short term stability [ppm** $2\times$**r.m.s.]**
RB	13000	10	0.8	0.4
RQ(D/F)	13000	10	0.8	0.4
RQX	18000	16	0.9	0.2
RTQX1	2000	2.09	1.1	1
RTQXA1	120[a]	3.32	27.7	5
RTQX3	2000	2.09	1.1	1
RCBX	2000	15	7.5	1
RQSX	200	4	20	2
RC(S/O)X	120	3	25	2
RC(D/T)X	120	3	25	2
RD(1/2)	13000	12	0.9	0.2
RCBRD	600	2	3.3	2
RQ(4/5)	6000	11	1.8	1
RCBY	120	0.67	5.6	5
RQ6	6000	13	2.2	1
RCBC	120	0.67	5.6	5
RTB8	300	1	3.3	2

[a] The rated current for this circuit has not been defined yet. The proposed value is compatible with the use of the trim.

Assuming the values computed in Table 27 as amplification factors for the beta-beating effect depicted in Fig. 14 and for the orbit effect depicted in Fig. 13 one can calculate the worst case scenario impact on beta beating and beam orbit (Δ) as:

$$\Delta = \sum_{i-\text{circuit}} |\Delta\tau_i \times \epsilon_i| \tag{26}$$

where $\Delta\tau_i$ are the delay-induced error from Table 27 and ϵ_i the single contribution of each circuit on beta beating or orbit. This calculation can be computed for any optics from injection to collision, however one can assume that the fully squeezed optics ($\beta^* = 15\,\text{cm}$) is the most sensitive to errors. The values obtained for such an optics are reported in Table 28. Note that this is a conservative scenario, in fact it corresponds to an hypothetical moment during the squeeze where all circuits are ramping and full speed and with delay errors set as such that the single effects do not compensate with each other, whit an optics that is already the fully squeezed one. All values computed in Table 28 seem to be well manageable and

Table 28: Expected maximum HL-LHC beam 1 orbit and beta beating error induced by the worst combination of the delay-induced error (See Table 27) for the 15 cm β^* optics.

	Horizontal	Vertical
Max IP1/5 orbit [$\sigma_{beam}10^{-2}$]	12.9	7.9
Max collimator orbit [$\sigma_{beam}10^{-2}$]	7.9	5.9
Max machine $\Delta\beta/\beta_0$ [10^{-3}]	6.6	6.4

correctable in the framework of tools and techniques already implemented for LHC operations.

For completeness, Fig. 15 shows the impact of each relevant circuit on beta beating along the whole machine at injection, to be compared with the equivalent plot for 15 cm β^* optics presented in Fig. 14. Note that at injection the impact is one order of magnitude smaller than at fully squeezed optics.

4.7 Summary

The current-control regime is driving the choice of the power converter class for the new HL-LHC circuits, while the dynamic aperture perturbation due to high frequency voltage tones might need to be reverified with simulations once new informations will be available, especially on the dumping effect of the beam screen.

A preliminary choice of PC class has been presented in Table 22. This choice allows for a minimal impact of the new PCs on the machine tune stability, which, as for the LHC, is the strongest constraint to allow for measuring and correcting the optics down to the level of 2 to 3% [35]. Still, the presently simulated performance would not allow to reach the target tune stability of 10^{-5} (see Table 23). If dedicated measurements will confirm such a behavior, a possible hardware improvement could be to upgrade of the ATS arcs main dipole PCs to class 0.

According to the present simulations, the impact on orbit of the PC's low frequency current jitter is negligible for standard operation (See Table 24). On a one-year long time scale the orbit stability is still dominated by other effects (e.g. ground motion), while it might become relevant the accumulated IP beta beating, which might become close to the 2.5% target precision for β^* measurements. Such an effect could be mitigated by regular calibration of the PCs or by dedicated optics adjustments over the year. Finally, the present ability of measuring and correcting the time delays between different circuits does not seems to pose any limitation to the adoption of ramp and squeeze also for HL-LHC.

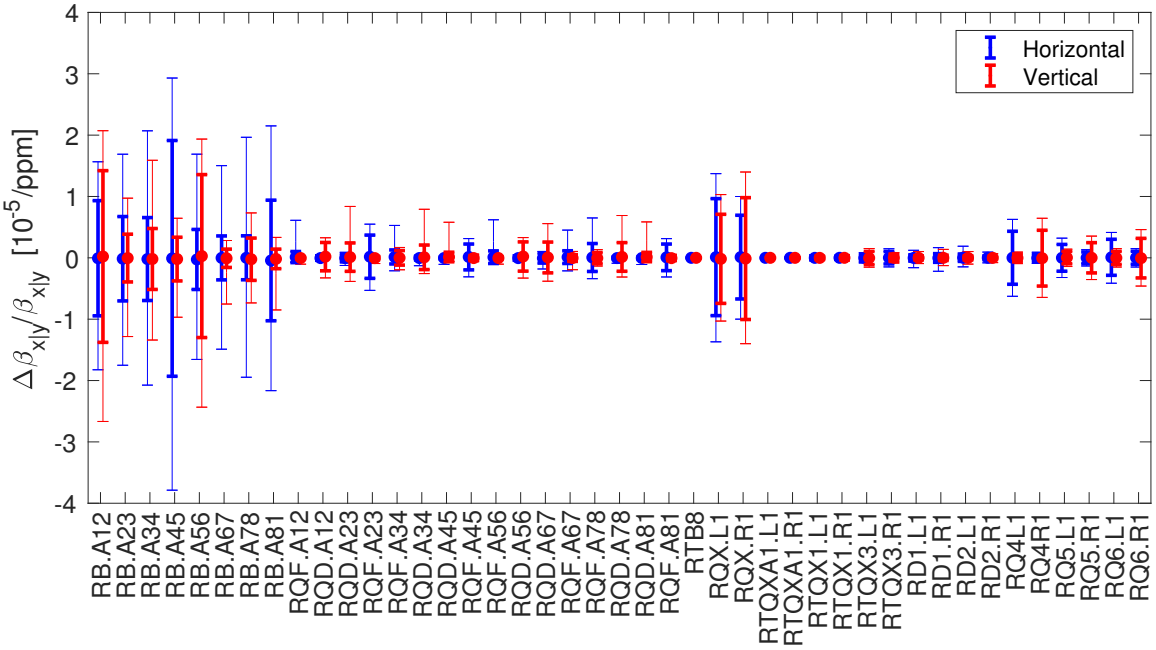

Fig. 15: Beam 1 beta beating along the whole machine under the effect of one ppm error on each relevant circuit of HL-LHC at injection optics (HLLHCV1.3). The thicker error bars give the mean and r.m.s. values, while the thinner error bars indicate the maximum excursion.

5 Summary and outlook

The analysis of the use of the current LHC circuits revealed that:

- The current ramp rates specifications are the fruit of years of operations, but are not strictly related to physical reasons.
- The driving parameter for choosing the ramp rates of new circuits has been identified in the speed of the main bending circuits.
- The ramp-down time of IR2 and IR8 triplets is the main obstacle for reducing the ramp down of the magnetic circuits (down to 25 minutes) and therefore the turnaround of the machine.
- The orbit correctors in the triplets are presently not used by the orbit feedback in order to avoid false-positive quench detections by the QPS, and consequent beam dumps.
- The uncertainty of all LHC PCs is considerably better than what initially specified in the LHC Design Report [2]. New quantities and definitions have been in Section 2.3 introduced to better describe the current performance.

Based on the observations of the a typical LHC cycle, and taking into account the new requirements of HL-LHC, specifications for the ramp and acceleration rates for the new HL-LHC circuits have been identified and summarised in Table 20. Those values take into account:

- the necessity of following the energy ramp, dictated by the speed of the main dipole PCs ramp rate (Section 3.1);
- preliminary thoughts on the impact of ramp-and-squeeze on the speed of triplets and relative trim circuits (Section 3.2);
- the needs for performing K-modulation (Section 3.4.1);
- the compensation of transfer function difference between 11 T dipoles and main dipoles (Section 3.4.2);
- the necessity of including the IR1 and IR5 orbit correctors in the orbit feedback, and the speed of the beam-beam orbit separation collapse (Section 3.4.3);
- the degaussing cycles for the non-linear correctors (Section 3.4.4).

The ramp-down time have been considered in Section 3.3. In order to maximise the possibility of reducing the turnaround time, it has been suggested to keep the ramp-down time of all new circuits below 1200 s, which is the ramp-down time of the main dipoles. It is also recommended to modify the triplet power converters in IR2 and IR8 to reduce their ramp-down time to at least 1500 s and to re-optimise the degaussing cycles of the different circuits that currently profit of the longer ramp-down time.

Considerations on the precycle have been made in Section 3.5. The assumed precycle length was fixed to 1800 s. Note that this have an impact on both the ramp rate and ramp-down time of 1-quad PC powered circuits.

The choice of the new PCs classes, Table 22, has been driven by the tight requirements on tune stability that affect β^* measurement and therefore the control of luminosity imbalance between IP1 and IP5. Simulations indicate that even in this case the necessary requirement of tune stability better than 10^{-5} is not fulfilled. The remaining dominant sources of noise are the main bend PCs of the ATS arcs. A campaign of new measurement in the LHC for confirming the results of our simulations is envisaged. If the above results will be confirmed, an upgrade to class 0 of the four PCs powering the main bents of the ATS arcs is recommended. This could also benefit the operation during Run III. On a one-year long time scale the chosen PC classes allow for a sufficient orbit and β^* stability at the low-beta IPs, even though the worst case scenario (see Table 25) is close to the limit of tolerable beta beating. In such a case possible mitigations have been identified in dedicated optics correction or PC calibrations during the year.

The present ability of synchronise the different circuits below 1 ms time error does not seem to pose problems to the implementation of ramp and squeeze (See Section 4.6). Also the long-term uncertainties (i.e. "stability during a fill (12 h)", "fill-to-fill repeatability" and "long term fill-to-fill stability") does not seem to be a major concern with respect to the acquired ability of measuring and correcting the LHC. An example is the orbit stability, computed in Table 24, that would remain below 1% of the beam sigma over a few fills. Larger variations are observed in operation (e.g. in [48]), probably due to ground motion effects. This suggests that other effects are dominant over the long-term uncertainties of the PCs.

Other uncertainty specifications are not fully established, yet. For example, the choice of the setting resolution for class 0 PCs has not been made yet. The presently proposed value of 0.5 ppm with respect to I_{rated} seems a reasonable starting point, but the impact on optics measurements needs to be assessed. The first studies of the effect of voltage ripple tones indicate that the amplitudes listed in Table 26 with the additional request of reducing the 300 Hz ripple amplitude by a factor 10 are sufficient to avoid significant effects on the DA. However, the recent development on modelling and measuring the influence of the beam screen might further relax this requirement [45].

Appendices

A Detailed plots on ramp and acceleration rates for LHC

Figure A.1 shows the extreme values of the current, ramp rates and acceleration rates achieved by different LHC circuits during the various beam processes for the fill #5848.

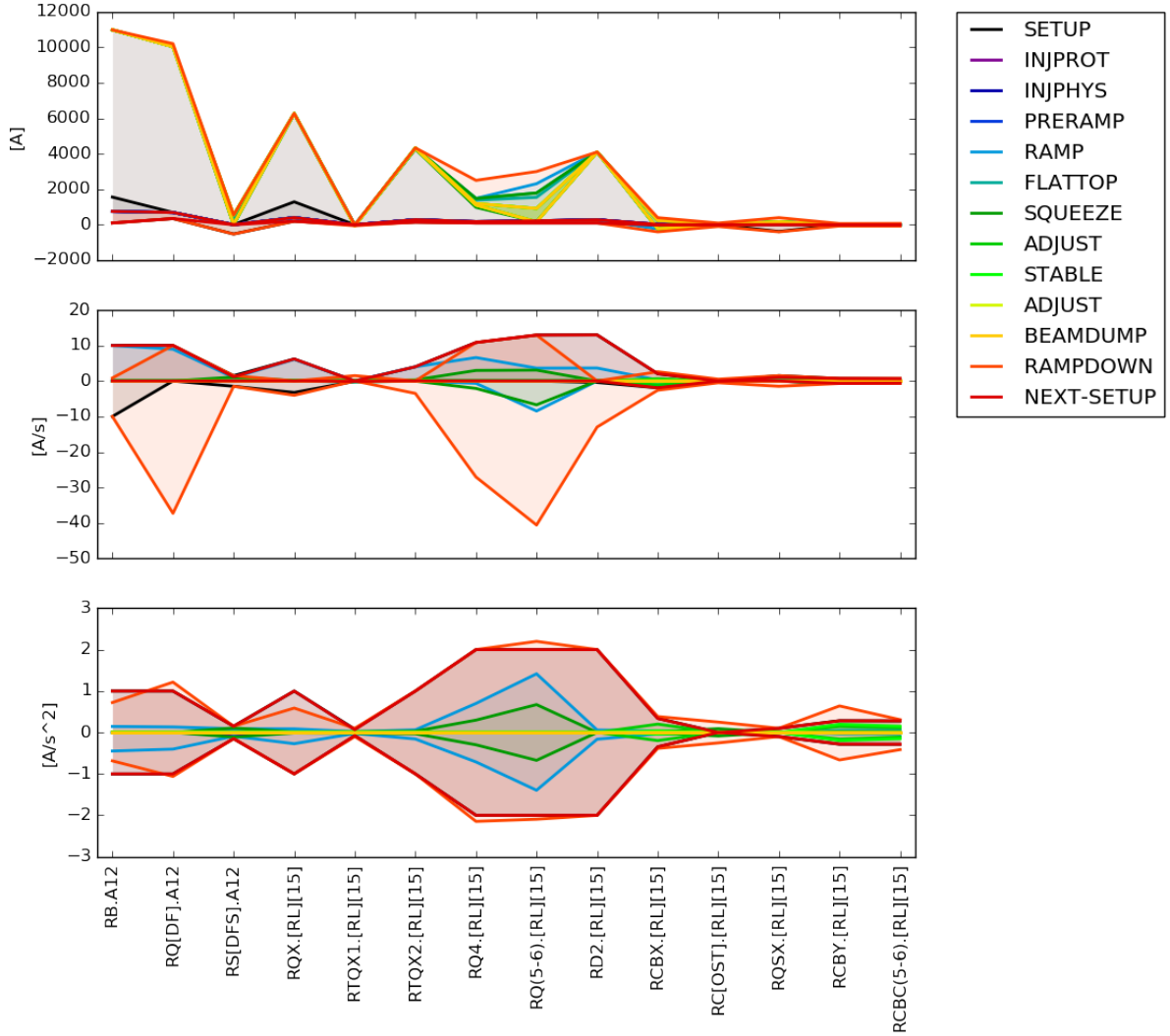

Fig. A.1: Maximum values of current, ramp and acceleration rates for various group of circuits during fill #5848.

B Use of LHC correctors

Figure B.1 shows the use of all orbit correctors in all IRs and relative matching sections during STABLE and ADJUST of fill #5848.

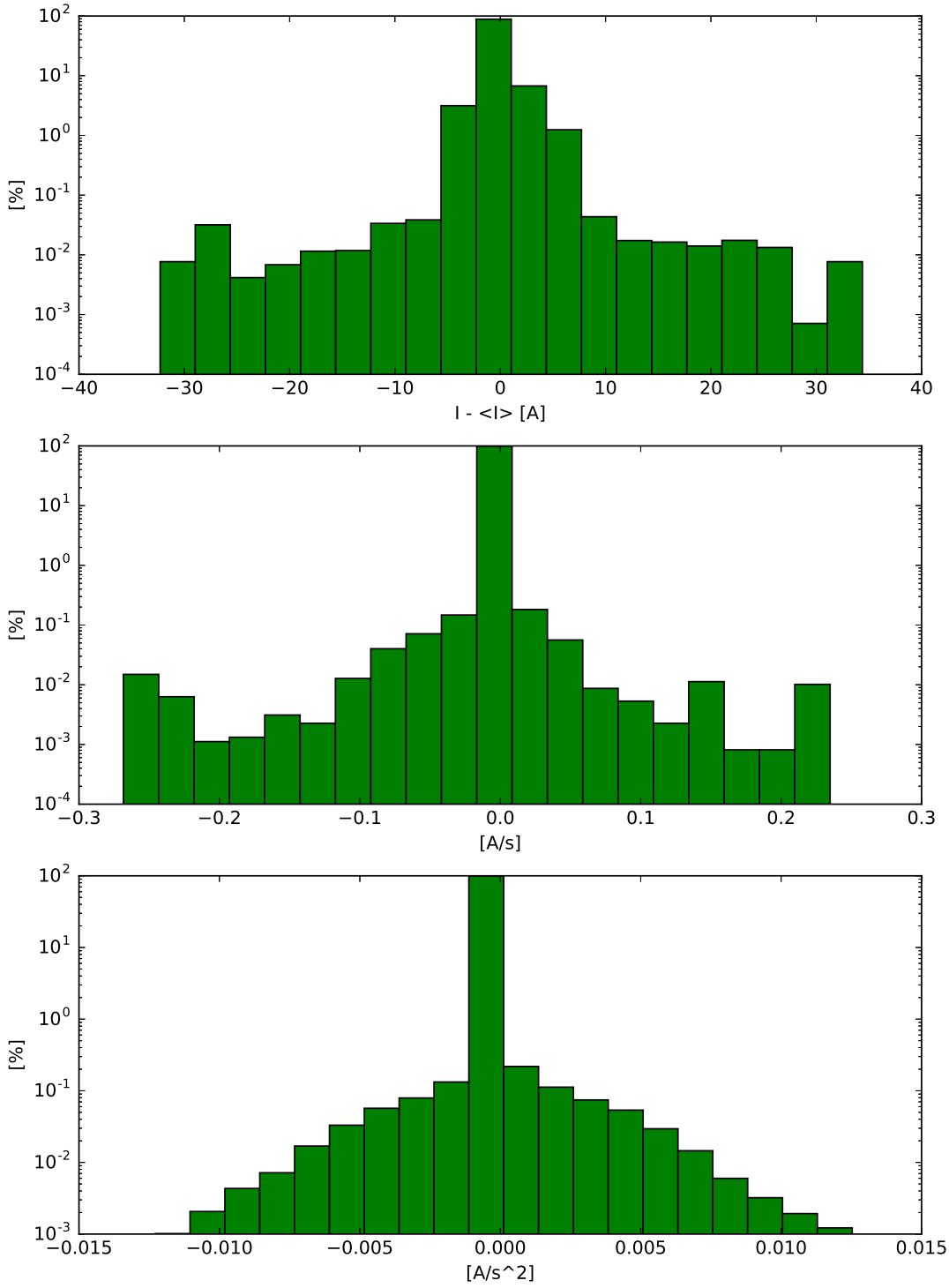

Fig. B.1: Histograms of the current variations (top), ramp rates (middle) and accelerations (bottom) for all orbit correctors in all IRs and matching section up to Q6 during ADJUST and STABLE beam operation of fill #5848. The current variation is computed with respect to the average current during the selected beam processes. All histograms are normalised to 100%.

C Scheme of the new HL–LHC circuits

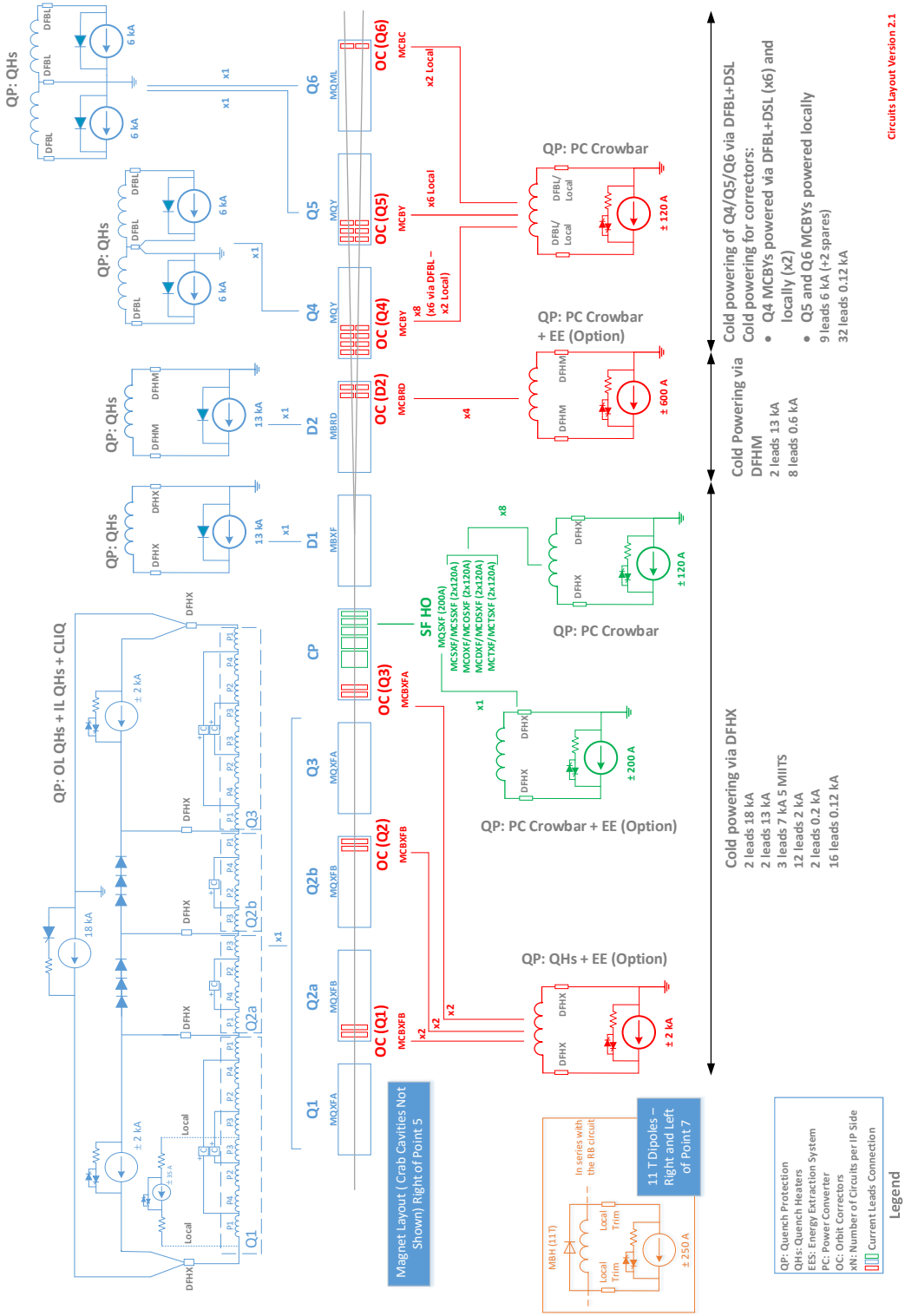

Fig. C.1: Layout of the new HL–LHC circuits, Version 2.1 [42].

References

[1] G. Apollinari, I. Béjar Alonso, O. Brüning, P. Fessia, M. Lamont, L. Rossi, and L. Tavian, "HL-LHC Technical Design Report," Tech. Rep. EDMS n. 1723851 v.0.71, CERN, Geneva, 2016.

[2] O. S. Brüning, P. Collier, P. Lebrun, S. Myers, R. Ostojic, J. Poole, and P. Proudlock, "LHC Design Report," Tech. Rep. CERN-2004-003-V-1, CERN, Geneva, 2004.

[3] S. Yammine, "HL-LHC Circuits Parameters, Version 7.2." `https://espace.cern.ch/project-HL-LHC-Technical-coordination/MCF/SiteAssets/Circuits\%20Table/Home/HL-LHC_CircuitParameters_HL-MCF_V7.2.xlsx`, October 2017.

[4] M. Pojer and M. Solfaroli Camillocci, "Parameters for LHC Superconducting Circuit Powering Tests," Tech. Rep. EDMS n. 1375861 v.1.2, CERN, Geneva, 2016.

[5] "CERN Layout Database." `https://layout.web.cern.ch`, June 2017.

[6] G. Arduini, B. Bellesia, J. Mariethoz, M. Pojer, M. Solfaroli Camillocci, A. Vergara Fernandez, and M. Zanetti, "Sector 2-3 powering specificities.," Tech. Rep. EDMS n. 883231 v.2.2, CERN, Geneva, 2009.

[7] "Twiki: circuits with known issues." `https://twiki.cern.ch/twiki/bin/viewauth/MP3/SummaryIssues`, September 2017.

[8] S. Fartoukh, "Achromatic telescopic squeezing scheme and application to the LHC and its luminosity upgrade," *Phys. Rev. ST Accel. Beams*, vol. 16, p. 111002, Nov 2013.

[9] P. Burla, Q. King, and J. G. Pett, "Optimization of the Current Ramp for the LHC," in *Proceedings of the 18th IEEE Particle Accelerator Conference, PAC99*, (New York, New York), Apr 1999.

[10] M. Solfaroli Camillocci. Private Communication.

[11] M. Solfaroli Camillocci, "LHC Operation and Efficiency in 2015," in *LHC Performance Workshop*, (Chamonix, France), January 2016. `https://indico.cern.ch/event/448109/contributions/1942062/`.

[12] R. J. Steinhagen, "LHC Beam Stability and Feedback Control - Orbit and Energy -," Tech. Rep. CERN-AB-2007-049, CERN, Geneva, 2007.

[13] J. Wenninger, "Implementation of crossing angle change," in *LSWG #18: MD results*, November 2016. `https://indico.cern.ch/event/581136/contributions/2361199/`.

[14] J. Wenninger. Private Communication.

[15] M. Cerqueira Bastos. Private Communication.

[16] Q. King, "Advanced uses of the WorldFIP fieldbus for diverse communications applications within the LHC power converter control system," in *Proceedings of the 10th International Conference on Accelerator and Large Experimental Physics Control Systems, ICALEPCS2005*, (Geneva, Switzerland), Oct 2005. WE4B.3-2O.

[17] O. S. Brüning, "Accelerator physics requirements at commissioning," in *Proceedings of the 11th LHC Workshop*, (Chamonix, France), 2001.

[18] R. Bailey, F. Bordry, L. Bottura, P. Burla, P. Collier, K. N. Henrichsen, J.-P. Koutchouk, R. J. Lauckner, R. Parker, J. G. Pett, P. Proudlock, H. Schmickler, R. Schmidt, L. Walckiers, and R. Wolf, "Dynamic effects and their control at the LHC," in *Proceedings of the 17th IEEE Particle Accelerator Conference, PAC97*, vol. C970512, (Vancouver, British Columbia, Canada), pp. 66–68, Jul 1997.

[19] M. Cerqueira Bastos, "High-precision performance of LHC power converters," in *2nd Workshop on Power Converters for Particle Accelerators (POCPA)*, June 2010. `https://indico.cern.ch/event/85851/contributions/1264219/`.

[20] M. Cerqueira Bastos, "Noise estimates for HL-LHC superconducting circuits," in *66th HiLumi WP2 Meeting*, April 2016. `https://indico.cern.ch/event/463032/contributions/1979653/`.

[21] M. Martino. Private Communication.

[22] H. Thiesen, M. Bastos, G. Hudson, Q. King, V. Montabonnet, D. Nisbet, and S. Page, "High Preci-

sion Current Control for the LHC Main Power Converters," in *Proceedings of the 1st International Particle Accelerator Conference, IPAC10*, (Kyoto, Japan), p. WEPD070, May 2010.

[23] "CERN TE-EPC-LPC Converter-Concepts / EMC." http://te-epc-lpc.web.cern.ch/te-epc-lpc/concepts/converters/emc/emc_emissions.stm, August 2017.

[24] R. De Maria, "Follow-up on orbit corrector requirements for IP and crab-cavity alignment," in *81st HiLumi WP2 Meeting*, November 2016. https://indico.cern.ch/event/572438/contributions/2379420/.

[25] M. Pojer. Private Communication.

[26] S. I. Bermudez, "DS-11T Dipole field quality version 5 February 2017." https://espace.cern.ch/HiLumi/WP11/Shared\%20Documents/field_quality.xlsx, February 2017.

[27] E. Metral, F. Antoniou, G. Arduini, P. Baudrenghien, N. Biancacci, C. Bracco, R. Bruce, X. Buffat, R. De Maria, D. Gamba, M. Giovannozzi, W. Höfle, G. Iadarola, N. Karastathis, A. Lasheen, K. Li, L. Medina, D. Mirarchi, P. Papadopoulou, Y. Papaphilippou, D. Pellegrini, S. Redaelli, G. Rumolo, B. Salvant, E. Shaposhnikova, M. Solfaroli-Camillocci, C. Tambasco, and D. Tomás, Rogelio Valuch, "Update of the HL-LHC Operational Scenarios for Proton Operation," Nov 2017.

[28] Q. King, "Analysis of time required for pre-squeeze and squeeze," in *Powering specification for HL-LHC*, February 2015. http://indico.cern.ch/event/369635/contributions/875363/.

[29] R. Tomás Garcia. Private Communication.

[30] R. De Maria, "Currents/Optics Transition in HL-LHC Circuit," in *55th HiLumi WP2 Task Leader Meeting*, September 2017. https://indico.cern.ch/event/676106/contributions/2772221/.

[31] R. De Maria. Private Communication.

[32] F. Carlier and R. Tomás, "Accuracy and feasibility of the β^* measurement for LHC and High Luminosity LHC using k modulation," *Phys. Rev. Accel. Beams*, vol. 20, p. 011005, Jan 2017.

[33] M. G. Minty and F. Zimmermann, *Measurement and control of charged particle beams*. Particle acceleration and detection, Berlin: Springer, 2003.

[34] J. M. Coello De Portugal, "Requirements of the Q1A trim," in *HL-MCF Meeting #18*, June 2017. https://indico.cern.ch/event/649566/contributions/2642171/.

[35] F. S. Carlier, J. M. Coello De Portugal Martinez Vazquez, E. Fol, D. Gamba, A. García-Tabares Valdivieso, M. Giovannozzi, M. Höfer, A. S. Langner, E. H. Maclean, L. Malina, L. E. Medina Medrano, T. H. B. Persson, P. K. Skowronski, R. Tomás Garcia, F. Van Der Veken, and A. Wegscheider, "Optics Measurements and Correction Challenges for the HL-LHC," Oct 2017.

[36] D. Wollmann. Private Communication.

[37] E. Todesco. Private Communication.

[38] C. Tambasco, "Specification of separation collapsing speed," in *67th HiLumi WP2 Meeting*, April 2016. https://indico.cern.ch/event/512381/contributions/2146006/.

[39] R. De Maria, "Specification of separation collapsing speed," in *Joint LARP CM26/Hi-Lumi Meeting at SLAC*, May 2016. https://indico.fnal.gov/event/11049/session/5/contribution/55.

[40] M. Solfaroli Camillocci, "Possible changes in precycle strategy," in *55th LHC Beam Operation Committee Meeting*, (Geneva), February 2016. https://indico.cern.ch/event/496880/.

[41] L. Bottura, M. Lamont, E. Todesco, W. Venturini Delsolaro, and R. Wolf, "Pre-Cycles of the LHC Magnets during Operation," Tech. Rep. CERN-ATS-2010-174, CERN, Geneva, Aug 2010.

[42] F. Rodriguez Mateos, "Magnet Circuit Forum SharePoint webpage." https://espace.cern.ch/project-HL-LHC-Technical-coordination/MCF, February 2017.

[43] "FiDeL home page." http://lhc-div-mms.web.cern.ch/lhc-div-mms/tests/MAG/Fidel/.

[44] M. Martino, "Modelling of the PC Output to the Magnetic Field," in *HL-MCF Meeting #7*, Novem-

ber 2016. https://indico.cern.ch/event/580993/contributions/2355718/.

[45] M. Morrone, M. Martino, R. De Maria, M. Fitterer, and C. Garion, "Magnetic Frequency Response of HL-LHC Beam Screens," October 2017. Submitted for publication.

[46] J. M. Coello De Portugal, "Minimum trim requirements and advantages of the single-circuit configuration," in *HL-LHC Magnet Circuits Internal Review*, March 2017. https://indico.cern.ch/event/611018/contributions/2476933/.

[47] D. Gamba and J. M. Coello De Portugal, "Impact of noise in the main LHC circuits – orbit, beta* and tune ripple," in *99th HiLumi WP2 Meeting*, July 2017. https://indico.cern.ch/event/655317/contributions/2668982/.

[48] J. Wenninger, "Machine reproducibility and evolution of key parameters," in *7th Evian Workshop*, December 2016. https://indico.cern.ch/event/578001/contributions/2366292/.

[49] M. Giovannozzi, "Operation and beam dynamics requirements," in *Conceptual Design Review of the Magnet Circuits for the HL-LHC*, March 2016. https://indico.cern.ch/event/477759/contributions/1156025/.